This paper is a non-peer reviewed preprint submitted to Geomorphology. The published journal article derived from this preprint has this DOI: 10.1016/j.geomorph.2022.108466

How cyclic processes determine fluvial fan formation and dynamics: Influence of eruptions on fluvial evolution and sedimentation in the Santa Clara Megafan, Costa Rica

Galve, J.P.[1]*, Alvarado, G.E.[2,3], Pérez-Peña, J.V.[1,4], Pérez-Consuegra, N.[5], Ruano, P.[1,6], Becerril, L.[7], Devoto, S.[8], Reyes-Carmona, C.[1,9], Azañón, J.M.[1,4,6]

[1]Departamento de Geodinámica, Universidad de Granada, Granada, Spain.

[2]Instituto de Investigaciones en Ciencias Geológicas, Universidad de Costa Rica, San José, Costa Rica.

[3]Unidad de Investigación y Análisis del Riesgo, Comisión Nacional de Prevención y Atención de Emergencias (CNE), San José, Costa Rica.

[4]Instituto Andaluz de Geofísica, Granada, Spain.

[5]Department of Earth, Atmospheric and Planetary Sciences, Massachusetts Institute of Technology, Cambridge, MA, USA

[6]Instituto Andaluz de Ciencias de la Tierra, CSIC-UGR, Granada, Spain.

[7]Instituto de Ciencias de la Ingeniería, Universidad de O'Higgins, Rancagua, Chile

[8]Dipartimento di Matematica e Geoscienze, Università di Trieste, Trieste, Italy

[9]Geohazards InSAR Laboratory and Modelling Group (InSARlab), Geoscience Research Department, Instituto Geológico y Minero de España (IGME-CSIC), Madrid, Spain

Abstract

Megafans are ever-evolving landforms and sedimentary bodies produced by rivers that regularly change their courses through avulsions. The processes that cause the avulsions and the rate at which the avulsions occur are tightly linked to the formation and evolution of themselves. The most common condition in their formation is high discharge (monsoonal) variability in the river that feeds the megafan. However, some megafans do not meet this condition, as in the case of the here studied, the Santa Clara Megafan in the tropical lowlands of Costa Rica. Its origin is related to active vulcanism which has determined a new setting for megafan development. This contribution presents new chronological, historical and remote sensing data to understand the temporal and spatial geomorphological evolution in this megafan during the last three millennia. We find that the evolution of the Santa Clara Megafan is related to the eruptions of the volcanoes where the megafan's source area is located. The major avulsions and shifts in the main rivers of the megafan are temporally and spatially correlated to strong eruptions (VEI $\geq$ 3) and a period with few changes in its fluvial system coincides with a less volcanic activity in the region. The megafan avulsion rate was estimated as 1 major avulsion per century in the last five centuries, when four strong eruptions (0.8 eruptions/century) took place. These changes in the rivers in response to the volcanic activity produced the activation or abandonment of megafan sedimentary lobes at a secular pace. The eruption cyclicity is also comparable to that of climate processes that control the evolution of megafans in other areas of the world but occurs at a different pace. Our review show that, in general terms, the formation of megafans is linked to cyclical exogenous or endogenous processes that produce the cyclical high sediment input events necessary to promote aggradation and frequent avulsions. Finally, the inferred geomorphological evolution of the Santa Clara Megafan has the potential to guide paleogeographical

reconstructions and archaeological studies and the collected avulsion history may be used for volcanic risk assessments in the studied region.

1. Introduction

Megafans are fan-shaped landforms composed of sandy and muddy sediments that cover more than 10^3 km^2 in area (DeCelles and Cavazza, 1999; Weissmann et al, 2010). They exhibit very low gradients (<1.5º) and a divergent fluvial system affected by recurrent avulsions (Latrubesse, 2015). Several authors have demonstrated the relationship between the behaviour and evolution of megafans with specific climate conditions. Leier et al. (2005), in the first global analysis of these features, stated that megafans are distributed in a belt that fringes the tropical climate zone (15-35° latitude). Subsequent studies (Weissmann et al., 2010, Hartley et al., 2010) show that their distribution is more extensive and mostly occur in regions of tropical and subtropical climates (Latrubesse, 2015) but they are also present at higher latitudes (e.g., 45°N in the Italian Alps; Fontana et al., 2014b). With regards to geological setting, the global distribution of megafans shows a special preponderance at the piedmont of active mountain fronts such as Himalayas (Gohain and Parkash, 1990), Alps (Fontana et al., 2014a; 2014b) and Andes (Horton and DeCelles, 2001). However, megafans are also present in other settings such as in intracratonic basins (e.g., Okavango – Botswana, Namibia, Angola–, Stanistreet and McCarth, 1993; Taquari –Brazil–, De Souza, 2002). Recently, a specific type of megafan related to active vulcanism has been described in a back-arc basin of the southern Central American arc-trench system: The Santa Clara Megafan (Galve et al., 2016). Avulsion of the channels in the Santa Clara Megafan appear to be controlled by volcanic eruptions, earthquakes and the intense hydrothermal weathering of volcanic rocks instead of high-discharge events in highly variable climate conditions as in other modern megafans (e.g., Leier et al., 2005). However, the specific mechanisms that control avulsions in the Santa Clara Megafan as well as the rates and timescales at which this megafan is being constructed remain poorly studied.

In this paper, we review the available chronological data and provide new dates and observations about geomorphic setting and events (e.g., river avulsions, channel migration) to describe with detail the evolution of the Santa Clara Megafan during the last three millennia. We follow the guide provided by Ventra and Clarke (2018) who summarized the current research on fluvial fans and megafans. These authors argue that to better understand the dynamics of megafans more geomorphological, hydrological and sedimentological studies focused on their boundary conditions, avulsion and flood histories and external influences are needed. Thus, we estimate the avulsion rate in the main fluvial channels of the Santa Clara Megafan and correlate avulsion events with the activity of the volcanoes that are the sediment source of the megafan. We compare the processes that cause avulsion, the rates of avulsion and general evolution of the Santa Clara Megafan with other well-studied non-volcanogenic megafans to extract generalized patterns on megafan formation and evolution worldwide. If the Santa Clara Megafan is controlled by volcanogenic processes it is expected that the fluvial landscape in this megafan has changed at a different pace than in other deeply studied megafans such as Kosi or Taquari megafans that evolve according to climate cycles (Chakraborty et al., 2010; Zani et al., 2012). Moreover, as Santa Clara is a particular example of megafan, we can provide information about aspects that may inspire explanation on the formation of other non-conventional megafans in the Earth and in other planets (e.g., Moore and Howard, 2005; Baker et al., 2015; Radebaugh et al., 2016). Furthermore, a better understanding of the sensitivity of the Santa Clara Megafan to volcanic perturbations has implications for archaeological interpretations and for volcanic risk assessments at regional and national scale, as discussed below.

2. Geological and geomorphological setting

The Santa Clara Megafan is situated in the lowlands of the Caribbean margin of Costa Rica (Figure 1), in the northern piedmont of the Cordillera Central, a mountain range formed by the biggest

93 volcanoes in Central America. The area is locally named the Santa Clara plains and is adjacent to the
94 Tortuguero coastal plain where the famous Tortuguero National Park is located (Figure 1).

95 Geologically speaking, the Santa Clara Megafan belongs to the North Limón Basin that
96 coincides with the piedmont of the Cordillera Central and Talamanca Cordillera, the Tortuguero plains
97 and the continental shelf. The North Limón Basin is an actively subsiding sedimentary basin formed
98 in the back-arc of the Central Costa Rica volcanic arc segment (Mende, 2001). The basin fill is
99 composed of a sequence that grades from deep-marine Late Cretaceous sediments to modern
100 continental volcaniclastic sediments representing a more or less continuous transition from pelagic to
101 continental conditions (Brandes et al., 2008 and reference therein). The Santa Clara Megafan forms
102 part of the younger sedimentary fill of the basin; with an age younger than 200 ka (Galve et al., 2016).

103 From a geomorphological point of view, the megafan is in a coastal plain developed between the
104 Cordillera Central and the Caribbean Sea. It is a fan-shape mega-landform of 1440 km^2 in area with
105 an approximate maximum length of 40 km (Galve et al., 2016). Technically, the Santa Clara Megafan
106 is not a conventional megafan because is formed by the coalescence of the alluvial deposition systems
107 of the Sucio, Chirripó, Toro Amarillo and Tortuguero rivers (Figure 1). According to the fluvial fan
108 classification of Zhang et al. (2020), the Santa Clara Megafan is a bending swinging-type fluvial fan
109 because the main cross rivers are meandering and it is form by two subfans (or sedimentary lobes).
110 The Santa Clara Megafan meets the conditions required to define it as a megafan because of its large
111 area, a clear fan morphology, the fluvial system show a divergent pattern, and it has a clear active
112 channel currently created by the convergence of the Chirripó Norte and Toro Amarillo rivers, which
113 has changed over time through avulsions. The anomalous direction of this active channel towards the
114 interior of Costa Rica's mainland instead of towards the Caribbean Sea (base level) was the first
115 evidence that Galve et al. (2016) notice to identify the megafan.

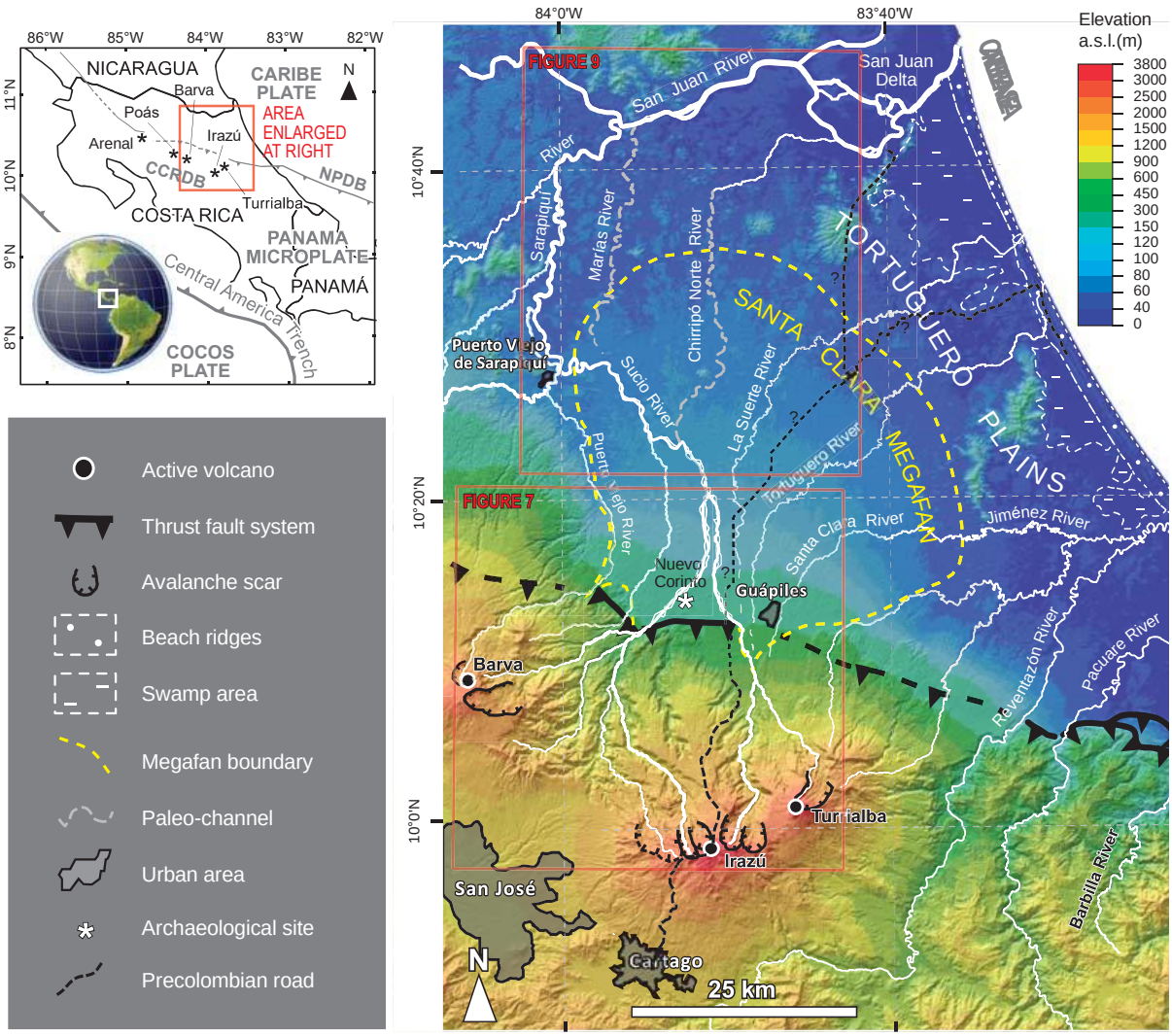

Figure 1. Location and geographical setting of the Santa Clara Megafan. NPDB: North Panama Deformed Belt; CCRDB: Central Costarrican Deformed Belt.

Regarding the surficial sedimentology, the fan body is composed of volcanoclastic sediments that grade from rounded boulders and cobbles, in the proximal area, to sandy, silty and clay sediments, in the middle and distal zone (Kesel and Lowe, 1987; Galve et al., 2016). Morphologically, Galve et al. (2016) differenced three main sectors: (1) a proximal zone that belongs to the alluvial apron of the Turrialba volcano that show braided channels and gradients from 10 to 30 m/km; (2) a middle segment with lower gradients (5-10 m/km) and braided to low-sinuosity meandering channels; and (3) a distal

part with a very low gradient (1-5 m/km) crossed by a divergent fluvial system of minor meandering streams with associated small ox-bow lakes and wide swamps.

A great part of the megafan surface is covered by soils developed in sandy volcanic sediments (Udands, Tropopsamments, Andic Dystropepts; Niewenhuyse, 1996). The soil map produced by Niewenhuyse (1996) for the region where the Santa Clara Megafan is located (Figure 2, Soil type: S3) shows how the distribution of these soils coincides with the terrains that surround the major channels of the megafan and encompass most of its area. The distribution of these soils reflects areas recently covered by sand sheets most probably associated to laharic activity of the last millennia (Niewenhuyse, 1996). These areas were our target for sampling and dating because they contain the sediments brought down from the volcanoes by lahars and can be related to avulsion processes.

The source area of the megafan sediments cover highly incised catchments developed in the Barva (2906 m a.s.l.), Irazú (3432 m a.s.l.) and Turrialba (3340 m a.s.l.) volcanoes (Figure 1). In one of these catchments, valley walls more than 1 km high were developed in less than 250 ka indicating a long-term fluvial incision rate among the highest on Earth (~5.6 m/ky; Galve et al., 2016). The processes behind these incredible incision rates are really a combination of endogenous and exogenous phenomena: (1) High rainfall produces great weathering of the bedrock and large flows in fluvial channels. (2) Ash fall from explosive eruptions increases erosion by killing the vegetation cover. (3) The sliding of slopes triggered by deep weathering of the bedrock due to hydrothermal activity and their destabilization caused by rainfall and earthquakes further maximized the abovementioned denudation processes (Galve et al., 2016).

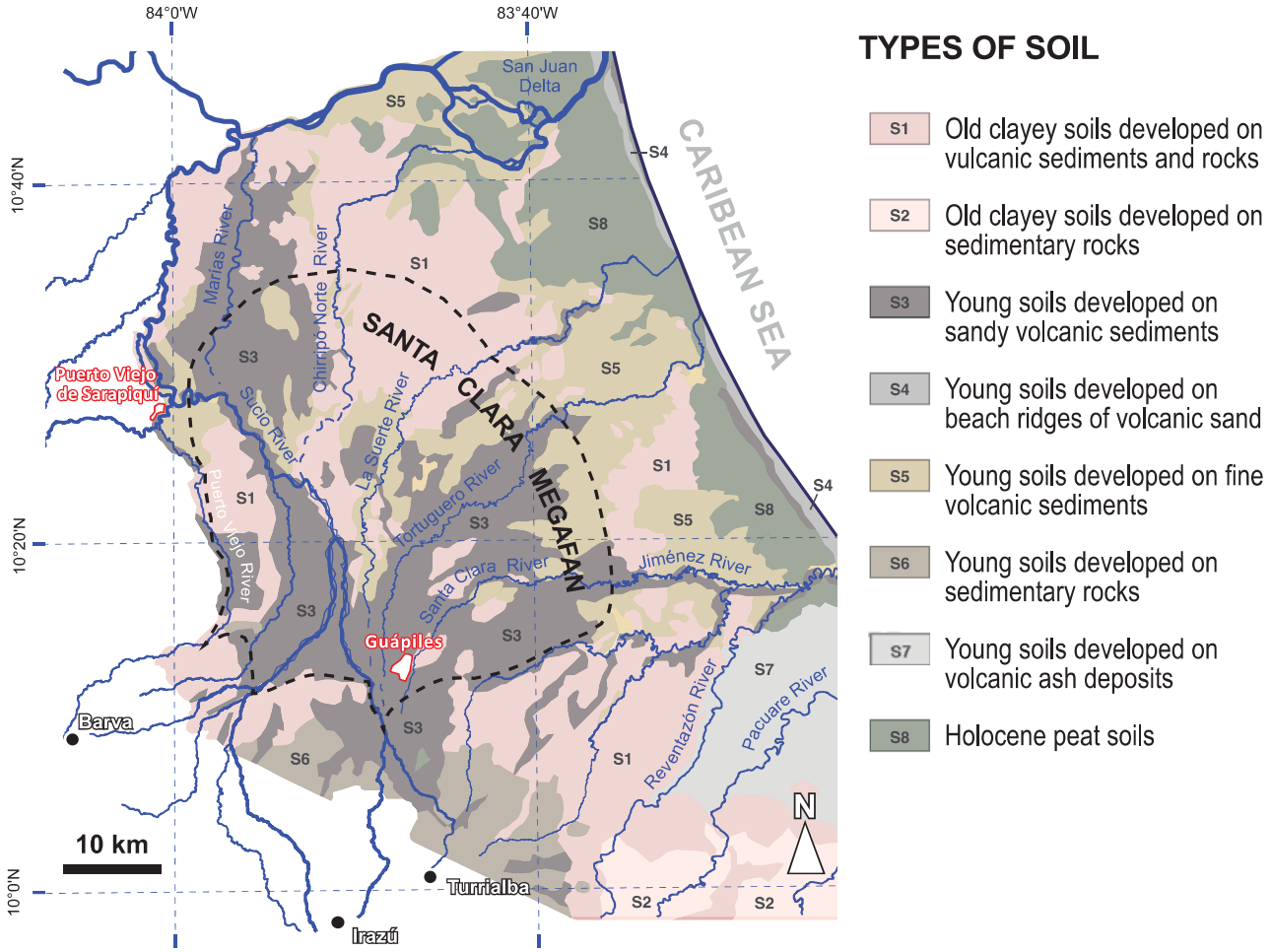

Figure 2. Soil map of the western sector of the Caribbean plains of Costa Rica (adapted from Niewenhuyse, 1996)

The modern climate in the Costarrican Caribbean lowlands is hot and humid with a mean annual temperature of 25°C and rainfall between 3.5 and 4 m (ICE, 2016). According to Koppën classification, the type of climate in the region is "Af", i.e. tropical rainforest climate. Two main seasons are usually identified in the area, the dry season from December to April and the humid season from May to November (ICE, 2016). The only difference between these seasons is the dry spells of days or weeks observed during the dry season. The megafan source area receives two times more precipitation than the lowlands. The Central Cordillera of Costa Rica has created an orographic barrier that concentrates

rainfall on its northern side generating extremely high values of mean annual rainfall up to 11 m (ICE, 2016).

3. Methodology

The region of the Santa Clara Megafan was considered a remote area just 150 years ago. Quoting directly from the map of Frantzius (1861), the area was considered "almost entirely unknown" in the middle of *s.* XIX. Therefore, there are not many historical records with enough detail to understand the dynamics of this region until the finale decades of the *s.* XX. The research work carried out by Kesel and Lowe (1987), van Seeters (1993), Nieuwenhuyse and Kroonenberg (1993), Dechesne (1994), van Ruitenbeek (1994) and Niewenhuyse (1996) were the first to explore the geomorphology of the Santa Clara plain and determine how fluvial dynamics have a certain relationship with the activity of volcanoes. We took this information as a base and, to go back further in the past, we planned a multi-approach research to study the changes in the megafan in the last decades, centuries and millennia. At decadal temporal scale, we analysed the NASA Shuttle Radar Topography Mission Digital Elevation Model (SRTM-DEM), images from Landsat and Sentinel 2 satellites, those available in public servers, and historical aerial photographs from the National Geographical Institute of Costa Rica (*Instituto Geográfico Nacional*, IGN). This information allowed us to study the changes in the megafan channels during the last decades in detail and, as we have been able to determine, during almost the last five centuries thanks to the recognition of many segments of paleochannels. To complete this study at centennial temporal scale, we examined historical maps, historical records and archaeological studies. We contrasted the information contained in historical documents with geomorphological evidences extracted from the available remote sensing (RS) data. The analysis of the RS data has been performed by direct observation of the images using different methods to enhance the contrast of them. The archaeological and geoarchaeological researches carried out by Salgado et

al. (2013, 2016) and Acevedo (2016) in the Santa Clara plains also provided important references for our interpretations about the geomorphic evolution of this region.

All the mentioned cabinetwork led to the selection of several sites that we inferred that they might represent critical places to understand the recent evolution of the studied fan. These sites are main avulsion points in the fluvial system and places where no chronological data were available so far. We performed several field surveys visiting these selected sites in order to describe them, to study sediment profiles and to take samples for dating the deposits through the radiocarbon method. This technique provided us with information at millennial scale. Finally, we integrate all the gathered information to contrast the observed evolution at different time scales with the processes driving the main changes in the fluvial system and to produce a geomorphological map. This map and all the compiled information help us in the understanding of all the landscape-modelling agents in the study area. We then elaborate a conceptual model of the Santa Clara Megafan's evolution in a decadal, secular and millennia scale.

3.1. Historic maps review

We carried out a comprehensive study of the historic maps of the Caribbean sector of Costa Rica. Table 1 lists the examined 13 historical maps (Table 1) with publications dates between 1625 and 1970 and other historical records that described fluvial processes (e.g. Peraldo and Mora, 2008). All these maps were analysed in detail taking several reference landmarks to compare the situation of the fluvial system in different periods of time. The older the maps are, the more inaccurate they are. On the other hand, the accuracy of the maps is not equal in all their sectors. However, all of them represent unique historical information to decipher the evolution of the megafan in the last five centuries. We corroborated with other historic sources (e.g. Ministerio de Fomento, 1885 and 1892) the credibility of the geographical features represented in them and what areas may be better defined because of human occupation and the interest and relevance of the region. Additionally, the review of the

mentioned historic documents shows us how place names have changed through time and this improved our interpretation of the maps.

Table 1. Historical maps reviewed.

Year	Author	Title	Extent
ca. 1625	Joannes De Laet	Nova Hispania, Nova Galicia, Guatimala	Central America
1671	John Ogilby	Yucatan Conventus Iuridici Hispaniae Novae Pars Occidenalis, et Guatimala Conventus Iuridicus	Central America
1764	Jacques Nicolas Bellin	Carte des provinces de Nicaragua et Costa Rica	Nicaragua & Costa Rica
1825	Philippe Marie Vandermaelen	Amer. Sep. No. 76. Partie Du Guatemala	Nicaragua & Costa Rica
1836	James Wyld	Guatemala or United States of Central America	Central America
1856	John Baily	Map of Central America	Central America
1861	Alexander von Frantzius	Originalkarte des nšrdlichen Theiles von Costarica, nach einer Original-Zeichnung	Northern Costa Rica
1868	Alexander von Frantzius	Mapa nuevo de Costa Rica	Costa Rica
1876	Luis Friederichsen	Carta geográfica de la República de Costa Rica (Centro América)	Costa Rica
1885	U.S. Coast & Geodetic Survey	East Coast of Central America From Cape Gracias A Dios To Gulf of Darien	Nicaragua, Costa Rica & Panamá
1890	Manuel María de Peralta y Alfaro	Mapa de Costa Rica, Veragua, Istmo de Panamá y Costa de Mosquito	Eastern Central America
1903	Henry François Pittier	Mapa de Costa Rica	Costa Rica
1970	US Department of Defense	Joint Operation Graphics 1:250,000 Sheet NC 17-5 Alajuela, Costa Rica; Nicaragua	Tortuguero coastal plain

3.2. Remote sensing methods and geomorphological map production

We used in this study all the RS data on hand that can provide useful information about the fan evolution (Table 2). Our objective was to map with as much detail as possible the past, recent and present fluvial network of the fan. The most used images to perform this task were those of high

209 resolution at the *IGN*, Bing™ and Google Maps™ servers. However, the exploration of those images
210 was primary guided by the analysis of medium-resolution Landsat and Sentinel 2 images (Table 2).

211 **Table 2.** Scene codes, satellite and date of the satellite images used to analyse the decadal and
212 secular evolution of the megafan channels

Scene	Satellite	Date
LT05_L1TP_015053_19911221_20170124_01_T1	LandSat 5	21/12/1991
LT50150531993040CPE00	LandSat 5	09/02/1993
LT50150531996321AAA02	LandSat 5	16/11/1996
LT50150531997355CPE03	LandSat 5	21/12/1997
LT05_L1TP_015053_19980919_20161222_01_T1	LandSat 5	19/09/1998
LT05_L1TP_015053_20000213_20161216_01_T1	LandSat 5	13/02/2000
LT05_L1TP_015053_20010114_20161212_01_T1	LandSat 5	14/01/2001
S2A T16PHS_20170126T160501	Sentinel 2	26/01/2017
LC80150532017026LGN01	LandSat 8	18/02/2017

213

214 A total of 8 relatively cloud-free Landsat images were obtained from the U.S. Geological
215 Survey Earth Explorer (http://earthexplorer.usgs.gov) database. One image was obtained from the
216 Sentinel 2 satellite from the European Union's Copernicus Programme. False color images were created
217 to generate enough contrast to visualize and identify different geomorphic features such as
218 paleochannels.

219 We also analysed (1) historic aerial photographs with stereoscopes to map and understand the
220 dynamics in the fan apex and to know how the landscape of the fan in the mid-20th century was; and

(2) the SRTM DEM to produce a geomorphological map of the fan where also the fluvial network recognized in satellite and aerial photographs was included. This map was also based on other geologic and geomorphological maps contained in the publications of Hidalgo et al., (2004), Pavanelli et al. (2004), Perez et al., (2006), Alvarado et al. (2006 and 2013), Ruiz Cubillo (2012), Alvarado and Vega (2013), Rojas et al. (2017) and Bergoeing (2018). The geomorphological map was digitised with QGIS 3.10 at a 1:25,000-scale and was used as primary source for the geomorphological interpretations. The chronological information described in the following section was also used in the map production.

3.3. Field survey and sample dating

The Santa Clara plains are hard to explore from a geological point of view. This is related to dense vegetation and cropland area mostly cover the plains (Figure 3A) and it is difficult to find good outcrops to recognize the subsurface deposits. Moreover, the information about boreholes in the region or other geological information about subsurface is difficult to obtain because it is on the hands of local private companies. We investigated the outcrops observed along river cutbanks and canals dug in banana and palm plantations (Figure 3B). In the middle and distal sectors of the fan, where the sediments are fine (i.e. sand, silts and clay), the upper 1-1.5 m of the studied profiles were disturbed by pedogenesis and we had to excavate and clean the outcrop using machetes, weeding hoes and Nejiri gama hoes to better observe the stratigraphy and sediment structures of the deposit. A total of 27 samples were collected from organic sediment and charcoal samples, of which we have were able to date 11 samples. Samples were sent to Beta Analytics® to obtain AMS radiocarbon ages and the ages were calibrated using CALIB 7.1.0 (Stuiver et al., 2018) and the data set IntCal13 (Reimer et al., 2013).

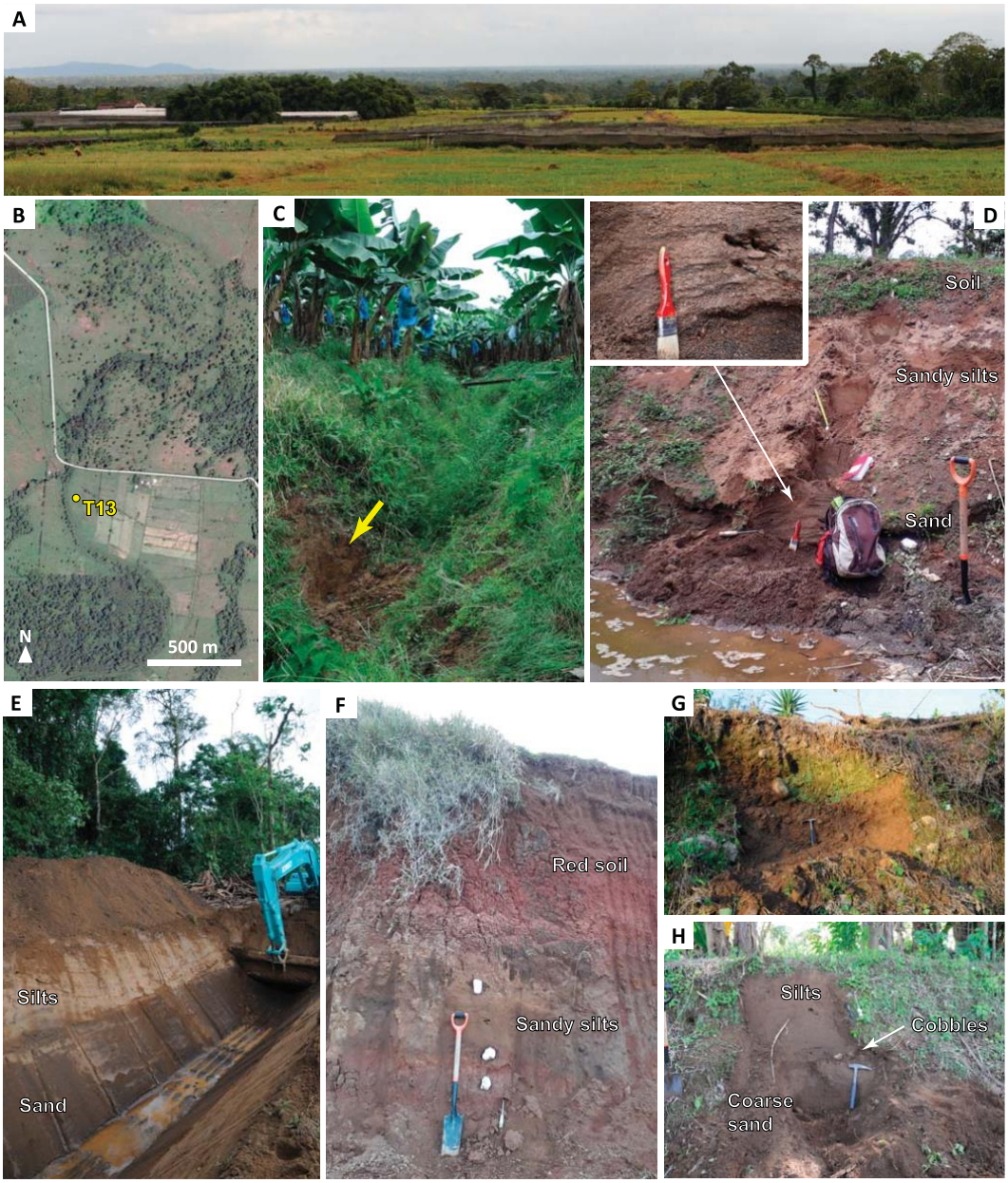

241

242 **Figure 3.** A. Landscape of the Santa Clara plains from the Turrialba apron. B. High-resolution
243 image from Google Earth® where the paleochannel of Marías River is easily recognisable. The
244 sample site of T13 sample is indicated. C. Example of sampling site (marked with a yellow arrow) in
245 a canal of a banana plantation. D, E, F, G and H. Field photographs of the sample sites of Mo-3, T13,
246 Mo-5, T06 and T04, respectively (see Figure 4 for the stratigraphic columns).

247

248

4. Results

We organized the results in two sections. First, we report the age of the dated sedimentary deposits and the relationship of these ages to events of geomorphic change in the Santa Clara Megafan. Second, we report geomorphological observations summarized in a detailed geomorphological map which incorporates the mentioned temporal information. These results will be integrated and interpreted in the discussion section.

4.1. Age of sediments and events in the Santa Clara Megafan

The stratigraphic columns and locations of the outcrops analyzed in this research are represented in Figure 4. The stratigraphic columns contain the location of the sampled datable material. The obtained dates are summarized in the Table S1 of the Supplementary material together with dates compiled from previous publications. The age of the deposits range from 150–15000 BC, therefore these results allow us to interpret depositional features and reconstruct the temporal evolution of the megafan on millennial to centennial timescales. The interpretations for each sample are included in the Table 3.

4.2. Geomorphological map of the Santa Clara Megafan

The 1:25,000-scale geomorphological map of the Santa Clara Megafan, which for publication purposes we divided in three figures presented below (Figures 7, 8 and 9), was produced by integrating all the information extracted from the satellite images, the interpretation of aerial photographs stereo pairs and the observations carried out in our field surveys.

Initially, the processing of Landsat images allowed us (1) to perform an analysis of decadal evolution; and (2) to identify older landscape features such as paleochannels that at some point crossed the Santa Clara plain.

We visually inspected the selected Landsat and Sentinel-2 scenes and looked-for paleo channel morphologies and depositional structures such as mid bars, side channel bars and scroll bars. The Landsat imagery in Figure 5 allowed us to observe several paleochannels morphologies. Also, we observed interannual variations (i.e., lateral channel migrations, avulsions, and formation of bars) in the modern channels of the fan.

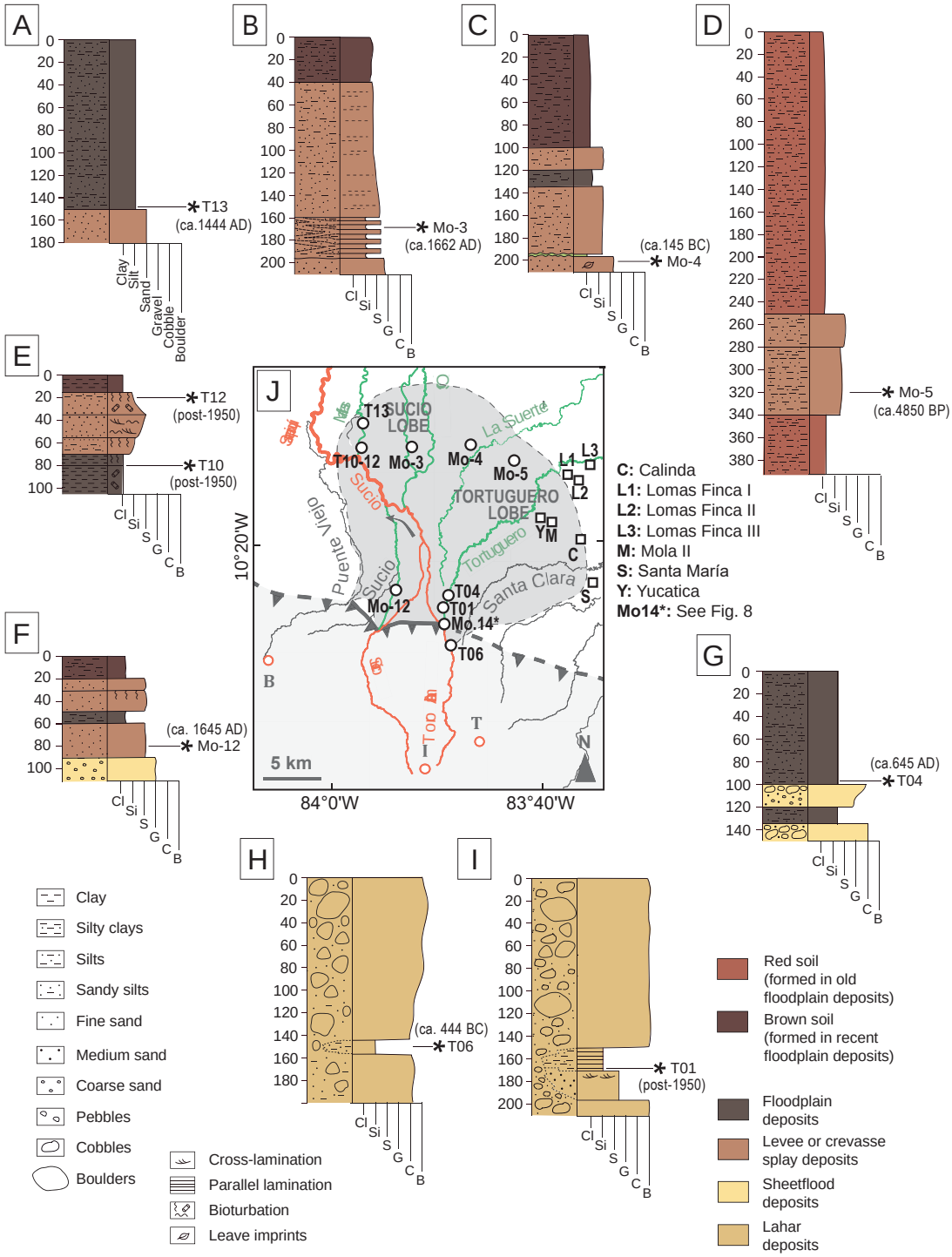

Figure 4. Stratigraphic columns of the sampled sites. The color of the rivers in panel J indicates the following: red rivers are current main channels of the megafan; green rivers are recent abandoned channels; and grey rivers are external channels from the current megafan fluvial system. In panel J has been located the C14 samples through their codes.

281 **Table 3.** Best estimate of the sample age and information interpreted from the stratigraphic setting.

Sample	Best estimate	Interpretation	Comment
T12 †	*s.* xx[2]	They date major floods in the final segment of Sucio River	
T10 †	*s.* xx[2]		
T01 †	*s.* xx[2]	They date lahars in the proximal lobe of the Toro Amarillo River.	This lahar is probably related to the 1970's avulsion event in the Chirripó River.
KL1*	*s.* xviii-xx[1]		This lahar could be related to the 1866 eruption of Turrialba or the 1723 eruption of Irazú.
Lomas Finca III	*s.* xvii *med.*-xviii	It post-dates a lahar or hyperconcentrated flow in the Tortuguero River.	Represents evidence of the full connection between the Toro Amarillo source area and Tortuguero River before *s.* XIX when this connection was progressively interrupted.
Mo-3 †	*s.* xvii *med.*	It dates a major flood in the west branch of the Chirripo River's old trace.	It indicates that this branch was active almost until this date.
Mo-12 †	*s.* xvii *med.*	It post-dates a major or a hyperconcentrated flow occurred in an old branch of the Sucio River in its proximal lobe (see Fig. 8).	It indicates that before this date this area was crossed by the Sucio River when this river was a major branch of the megafan.
KL2*	*s.* xii *in.*-xvii	It dates a lahar in the proximal lobe of the Toro Amarillo River.	This lahar is could be related to the 1561 eruption of Irazú.
T13 †	*s.* xv *med.*	It post-dates one of the last major floods in the Marías River.	It indicates that before this date Marías River formed a major fluvial channel of the megafan, probably connected to the Sucio River. This date seems to be just before its abandonment.
T04 †	*s.* vii *med.*	It post-dates a minor lahar in the proximal lobe of the Toro Amarillo River in an area connected with the Tortuguero River.	It seems to indicate that before this date Tortuguero River was a major fluvial channel in the megafan and it was fully connected with the Toro Amarillo source area.
Mo-4 †	*s.* ii-i[1] b.c.	They pre-date hyperconcentrated flows in the Tortuguero lobe.	They reveal that after these dates there was full connection between the Toro Amarillo source area and the Tortuguero lobe and it occurred a major event of sedimentation in this lobe because all dates are similar but they are distributed widely over the eastern part of the megafan.
Yucatica SF1	*s.* iv-i[1] b.c.		
Mola II	*s.* iv-i[1] b.c.		
Calinda	*s.* iv-i[1] b.c.		
Yucatica SF2	*s.* vi-iv b.c.		
T06 †	*s.* v b.c.	It dates one of the last lahars in the old apex of the megafan (see Fig. 8).	It pre-dates the abandonment of this part of the megafan and the migration of the apex to the current position most likely between *s.* V BC and *s.* I.

Sample	Best estimate	Interpretation	Comment
Lomas Finca I	*s.* viii-v b.c.	They post-date hyperconcentrated flows in the Tortuguero River.	They reveal the full connection between the Toro Amarillo source area and the Tortuguero lobe during this period. The associated lahars are may be related to the ca. 695 BC eruption of Irazú or the ca. 1200 BC eruption of Turrialba. However, uncertainty in the dates prevents to associate more clearly this sediments to these eruptions.
Yucatica BSFZ 2	*s.* viii-v b.c.		
Santa Maria	*s.* xv-x b.c.		
Yucatica BSFZ 1	*s.* xv-x b.c.		
Mo-5 †	~4850 BP	It dates a hyperconcentrated flow in the Tortuguero lobe below old red soils.	It reveals that the red hills observed in the megafan are more recent than it was previously thought.
KL3*	~12500 BP	They date lahars in the old apex of the megafan.	This date can be used to estimate sedimentation rates in the apex.
KL4*	~12000 BP		
Mo-14 †	~17200 BP		

* Samples with a imprecise location (see Kesel and Lowe, 1987).

† Samples dated in this study.

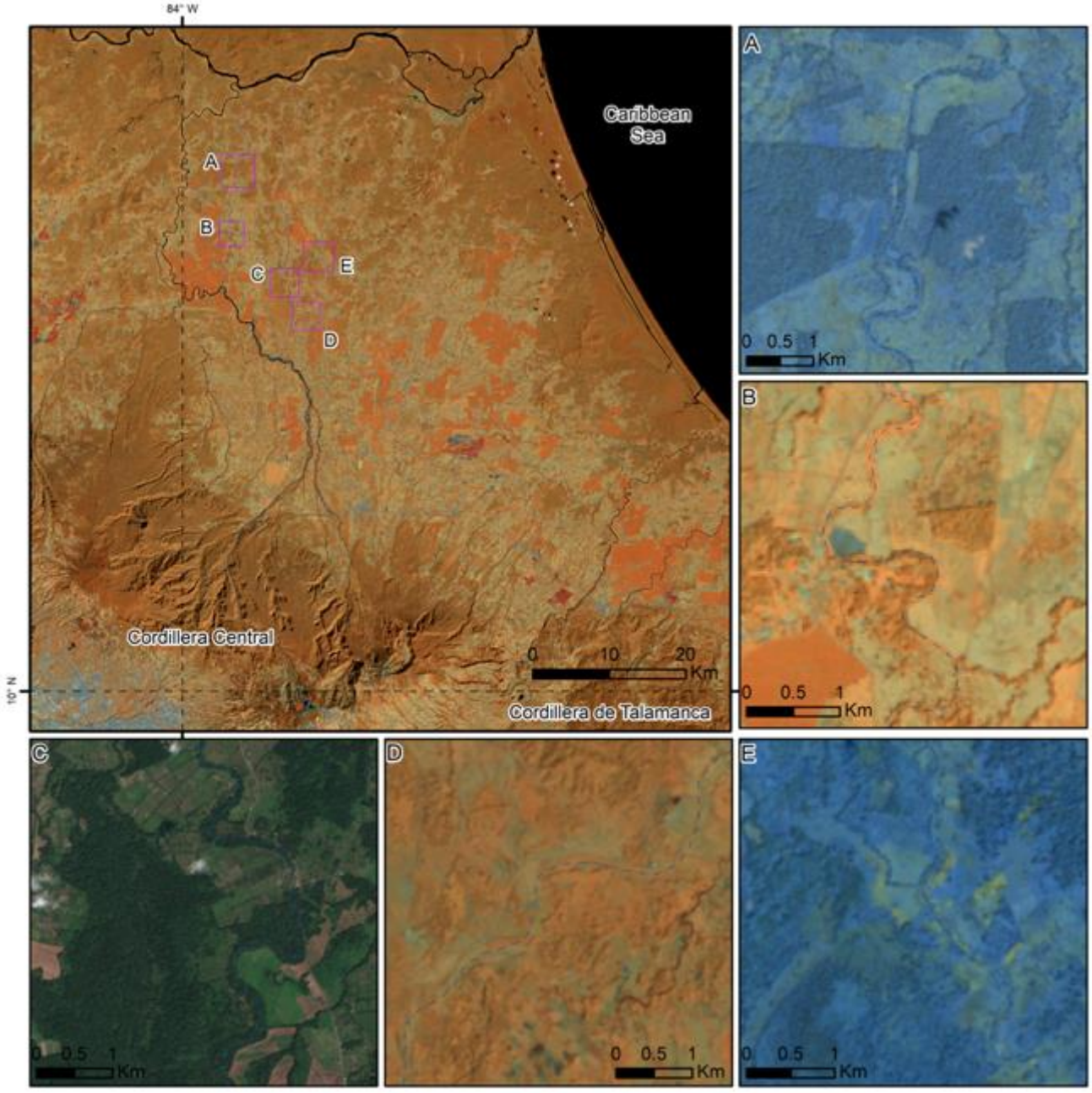

Figure 5. Examples of different observations carried out using satellite images. The upper left panel is a Landsat image of 1997 with a 456 band composition that cover the region of the Santa Clara Megafan and serve as reference to locate the other frames (See Table 4 to know the details of the panels in the right and in the bottom)

Figure 6 shows a sequence of Landsat scenes that demonstrate interannual variability in the position of the river channels during the 1991–2017 interval in the Sucio River. Table 4 include information about the satellite, date, band composition and observed features showed in Figure 5.

From this satellite imagery we have recognized how the Sucio River migrated laterally only within the channel belt (Figure 6). The Landsat scenes evidence lateral channel migration and scroll bar formation. Also, the river repeatedly has small avulsions during the period of 26 years covered by the satellite imagery. The flow is usually diverted into a new channel during flood events, abandoning the old meander or producing an anabranching pattern.

Figure 7 shows the megafan source, apex and proximal area. One feature that stands out in the map is the great fluvial erosion developed in the east sector of the Barva volcanic edifice and the west sector of the Irazú volcano, which mostly corresponds to the Sucio River Basin. Therefore, this basin seems to be the main sediment source of the megafan and Sucio River should correspond to the main channel. Several active faults also cross the Sucio River Basin (Figure 7A) and they contributed in the fracturing and weakening of the bedrock favouring erosion. Moreover, the earthquakes produced by these faults also may enhance erosion causing the destabilization of the slopes and this can explain the great incision and the near absence of planèzes in that sector.

The map also shows several scars of debris avalanches. Their abundance may explain why the source area has produced the high sedimentation rate needed to create the megafan. The freshest scar is the one located in the west flank of Irazú where two large failures occured in 1994 (Fallas et al., 2018) and 2020 and continue to be unstable (Muller et al., 2021). Before these landslides, the most recent scar generated by a volcano flank collapse is the one where the Turrialba Volcano's main craters are situated. However, although this has an estimated age between 62 ka and 9 ka, according to the data extracted from the report of Alvarado et al. (in prep.), the slide body has already been obliterated by lava flows and subsequent fluvio-volcanic sedimentation. This reflects the intense activity of volcanic

311 and surface processes in the region. In the other cases, debris avalanche crown scarps are the only
312 remain of gigantic mass movements and currently they have become headwaters of the main rivers
313 that feed the megafan area. The combination of fluvial erosion with debris avalanches may explain the
314 great long-term incision rates (~5.6 m/ky) calculated in the area (see Galve et al. 2016). Therefore,
315 these rates include fluvial incision and also hillslope processes of large scale as mentioned before (see
316 section 2).

317 **Table 4.** Satellite, date of the image, band composition and description of the panels in the Figure 5.

Figure panel	Satellite	Date	RGB Bands	Description
A	Landsat 5	21/12/97	6,5,4	Paleochannel of the Marías River
B	Landsat 5	14/01/01	4,5,6	Idem.
C	Sentinel 2	26/01/17	4,3,2	W branch of the Chirripó River (paleochannel)
D	Landsat 5	21/12/91	4,5,6	E branch of the Chirripó River (paleochannel)
E	Landsat 5	21/12/97	6,5,4	Idem.

318

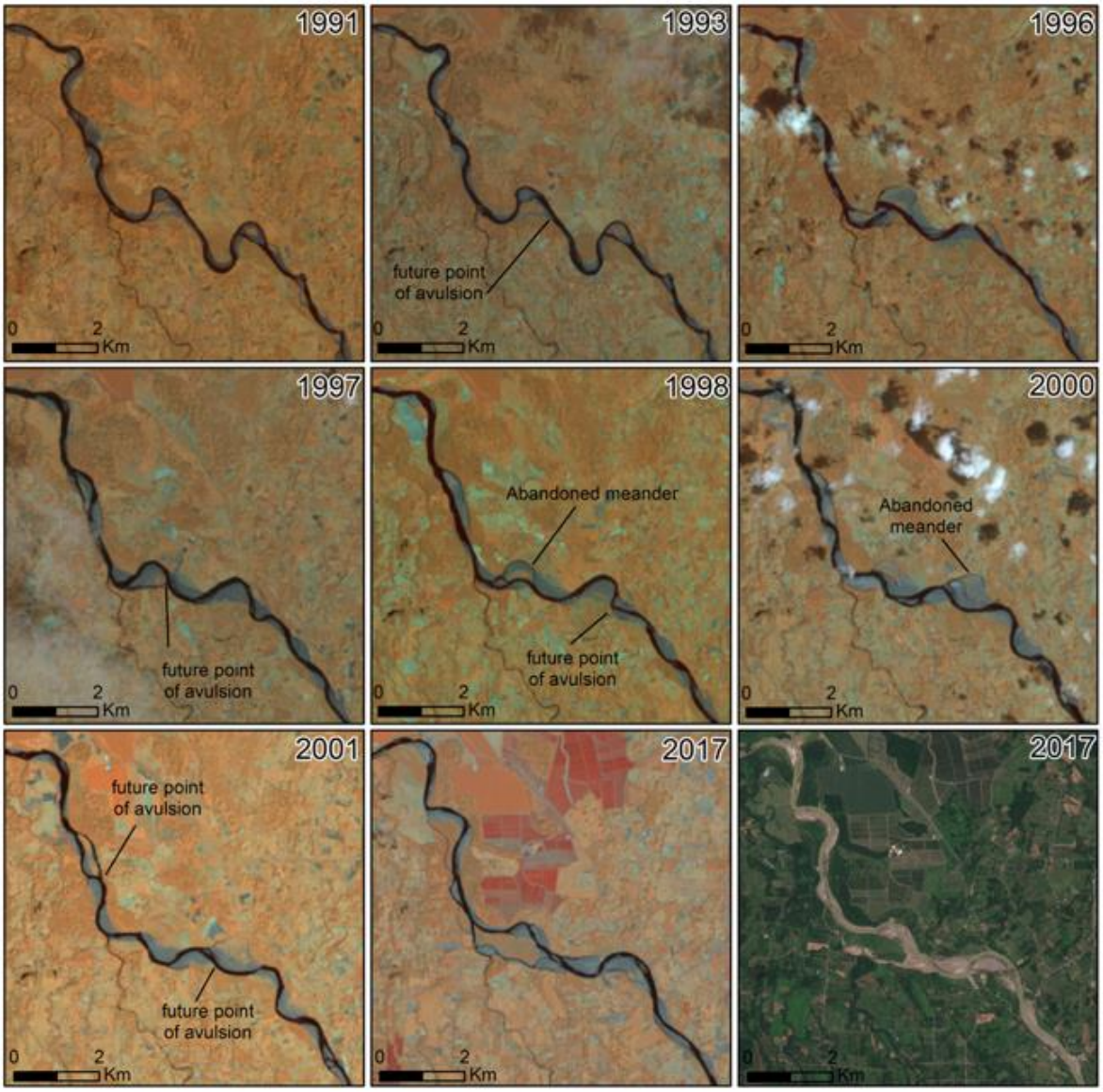

Figure 6. Decadal evolution of the Sucio River from 1991 to 2017. Images with false color composition are Landsat images (RGB bands: 456). The lower right panel is a Sentinel 2 images with a band composition 432.

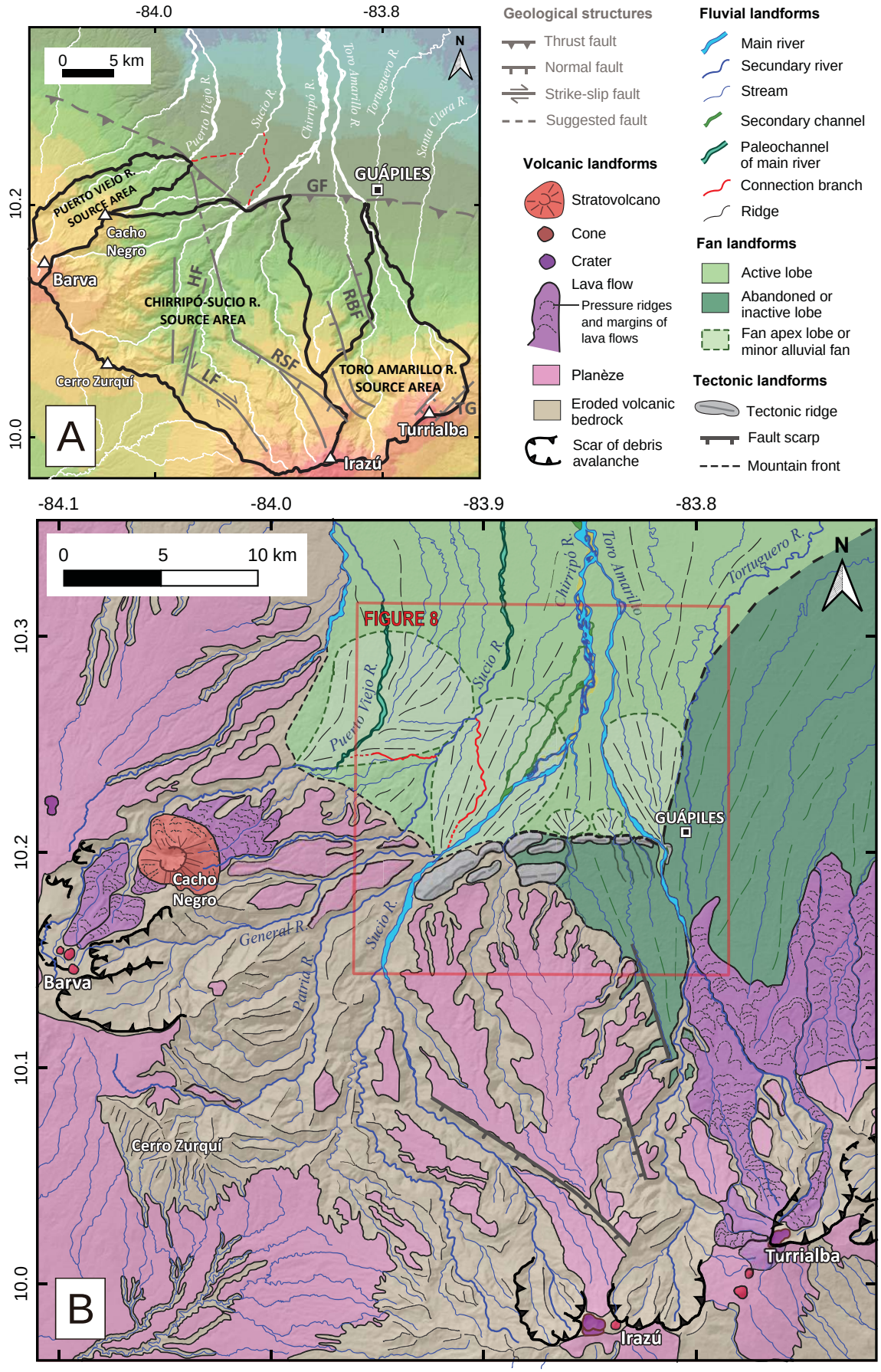
-84.0
-83.8
0 5 km
N
Puerto Viejo R.
Sucio R.
Chirripó R.
Toro Amarillo R.
Tortuguero R.
Santa Clara R.
GUÁPILES
GF
PUERTO VIEJO R. SOURCE AREA
Cacho Negro
Barva
HF
CHIRRIPÓ-SUCIO R. SOURCE AREA
RBF
RSF
LF
TORO AMARILLO R. SOURCE AREA
TG
Cerro Zurquí
Turrialba
Irazú
A
10.2
10.0
Geological structures
Thrust fault
Normal fault
Strike-slip fault
Suggested fault
Volcanic landforms
Stratovolcano
Cone
Crater
Lava flow
Pressure ridges and margins of lava flows
Planèze
Eroded volcanic bedrock
Scar of debris avalanche
Fluvial landforms
Main river
Secundary river
Stream
Secondary channel
Paleochannel of main river
Connection branch
Ridge
Fan landforms
Active lobe
Abandoned or inactive lobe
Fan apex lobe or minor alluvial fan
Tectonic landforms
Tectonic ridge
Fault scarp
Mountain front
-84.1
-84.0
-83.9
-83.8
0 5 10 km
N
FIGURE 8
Chirripó R.
Toro Amarillo
Tortuguero R.
Sucio R.
Puerto Viejo R.
GUÁPILES
Cacho Negro
General R.
Sucio R.
Barva
Patria R.
Cerro Zurquí
Turrialba
Irazú
B
10.3
10.2
10.1
10.0

323

Figure 7 (previous page)**.** A. Source areas of the Santa Clara Megafan and geological structures. GF: Guapiles Fault; RBF: Río Blanco Fault; RSF: Río Sucio Fault; LF: Lara Fault; HF: Hondura Fault; TG: Turrialba graben. B. Geomorphological map of the megafan source area. Note that there are two rivers with the same geographical name: Sucio River. We infer that this river channels were connected in the past forming one of the main channels of the megafan.

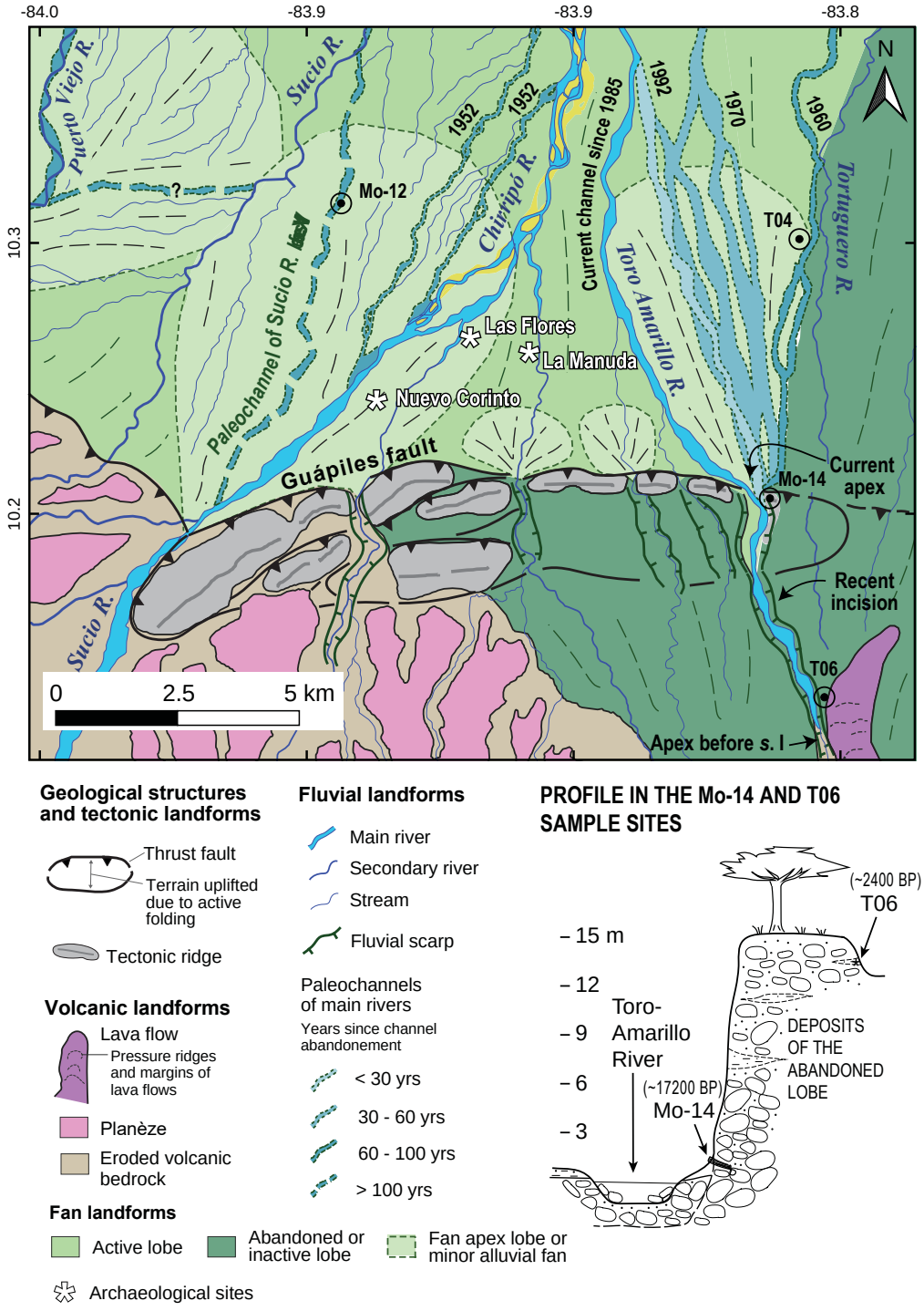

Figure 8. Geomorphological map of the megafan apex. Dates next to paleochannels indicate the last registered date these channels were active.

Another aspect to highlight in the map is the current inactive sector of the fan (i.e. eastern sector; Figure 7), probably abandoned due to river shifts related to lava flows and other volcanic perturbations. This sector seems to coincide with an old apex of the megafan (Figure 7). The ground uplift caused by the Guápiles Fault activity could be also the cause of the disconnection of this apex from the rest of the fan. Those issues will be accounted in the following description of the Figure 8.

Figure 8 focuses on the apex of the megafan where many geomorphic changes have occurred in the last millennia. There are three proximal lobes acting as minor fans inside the megafan. In present times, the main proximal lobes are formed by the Sucio-Chirripó and Toro Amarillo rivers, while the Puerto Viejo River forms a smaller fan on the western side. The map illustrates how the fluvial channels of those rivers have evolved through a recent confluence. On one hand, the channel of the Sucio-Chirripó River has migrated 5 km to the east in almost the past 300 years (Figure 8). The eastward migration of the Sucio-Chirripó River was recognized by detecting several paleochannels to the west of the modern channel using satellite imagery and dating the westernmost paleochannel to ca. 1645 AD (Sample Mo-12, Table S1). On the other hand, the channel of the Toro Amarillo River migrated 3-4 km from east to west during the second half of the *s.* XX. The westward migration of the Toro Amarillo River was also recognized by detecting several paleochannel to the east of the modern channel using satellite imagery and dating the easternmost paleochannel using historic aerial photographs. The westward migration of the Toro Amarillo River has caused a great change because at ca. 645 AD the Toro Amarillo River poured its water into the Tortuguero River (Sample T04, Table 3) that runs onto the Caribbean Sea and now the Toro Amarillo River flows onto the Sucio-Chirripó River that instead runs westward.

Figure 9 shows the NW sector of the Santa Clara Megafan, which is the area that has seen the most geomorphic changes in the fluvial system in the last centuries. In this map we delineated the trace of the main channels of the megafan on the past five centuries. An interesting aspect about this

357 map is to see how we have been able to recognize fluvial channels older than several centuries and the
358 rapid evolution in this sector during this time.

359 Here, to better describe the map in Figure 9, it is important to link the map with some
360 radiocarbon dates. We determined that the Sucio River was not connected to Sarapiquí River before
361 the *s.* XV. Instead, the Sucio River was connected to the Marías River five hundred years ago forming
362 the main channel of the Santa Clara Megafan at that time (orange trace/paleochannel in Figure 9). The
363 evidence for the Sucio–Marías connection is derived from an age of ca. 1441 AD on the paleochannel
364 and from satellite imagery.

365 The multiple avulsions of the ancient Sucio River channel created an area plenty of
366 disconnected paleochannels in the Caño Negro area (Figure 9) that seems to indicate that the fluvial
367 system migrated rapidly from the West to the East, leaving many interconnected paleochannels, and
368 finally the Sucio River was transformed into the present Chirripó River converging with the Toro
369 Amarillo River (Figure 8). The Chirripó River continued this displacement eastward and abandoned
370 another branch in the *s.* XVIII (yellow trace in the Figure 9) located to the west of the Cerro Negro. In
371 the *s.* XIX, the Chirripó River (green trace in the Figure 9) was located east of the Cerro Negro. We
372 inferred the location of the Chirripó River in the *s.* XIX from historical maps that show that its former
373 position was used to delineate the border between the Costa Rican provinces of Heredia and Limón.
374 Nowadays, the Chirripó River does not flow there but the political border that separates the provinces
375 remains, and it is a witness of the old river trace. In AD 1970 a great avulsion diverted the Chirripó
376 River to the West (Nieuwenhuyse et al., 1996) as it stands at present. During our field surveys we
377 determined that most of the people living today in the region have forgotten about the former location
378 of the river prior to the 1970 avulsion.

379

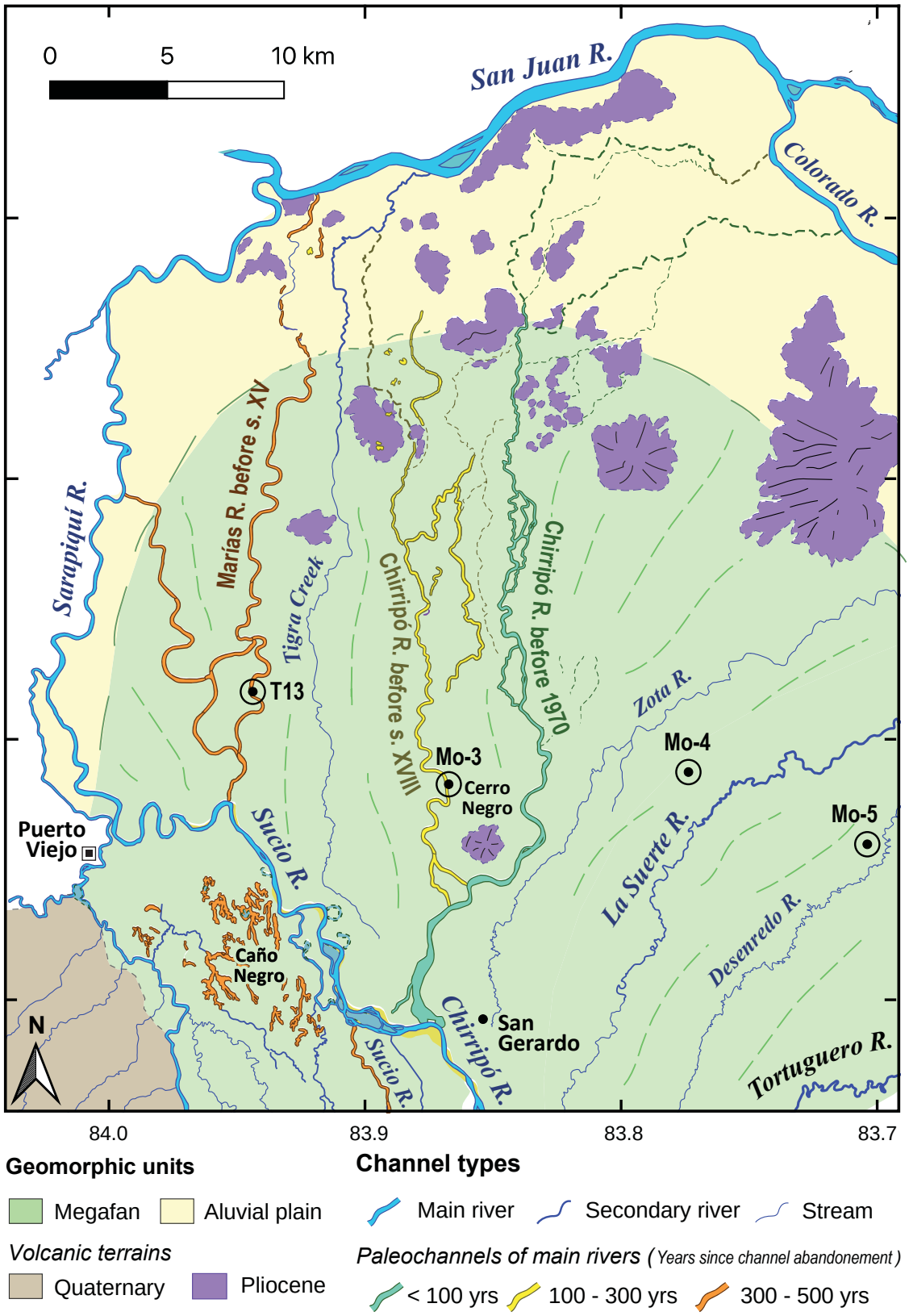

380

381 **Figure 9.** Geomorphological map of the western sector of the megafan

382 **5. Discussion**

383 **5.1. Driving forces behind the landscape changes in the Santa Clara Megafan**

384 Galve et al. (2016) defined a conceptual model to explain the formation and temporal evolution
385 of the Santa Clara Megafan. The model was based on insights from previous authors (Vessell and
386 Davies, 1981; van Ruitenbeek, 1994; Pierson et al., 2014) and their own observations and calculations
387 on the sediment budget between the erosion and deposition in the megafan source-sink system (see
388 Galve et al., 2016 Supplementary Material). Galve et al. (2016) argue that endogenic processes (i.e.
389 volcanic activity) control Santa Clara Megafan evolution at millennial timescale. Active volcanism is
390 the dominant process that triggers the greatest changes on the fan and as well as explaining its
391 formation. Secondary processes include active tectonics and landsliding enhanced by rock fracturation
392 and hydrothermal weathering and triggered by eruptions and earthquakes. The model of Galve et al.
393 (2016) was a good starting point to understand the processes that control the geomorphic evolution of
394 the Santa Clara Megafan, however, the model needed additional evidence on the rates of geomorphic
395 change to improve its robustness. In this contribution we complement the existing model by describing
396 the evolution of the megafan fluvial system and constraining the rates of the geomorphic change
397 associated.

398 The dates of the sampled sediments, despite their uncertainties, show spatial and temporal
399 patterns from which to deduce major changes in the configuration of the megafan during the last three
400 millenia (Figure 10). The temporal and spatial resolution of our data improved as we approach the
401 present. Thus, we have a clearer picture of the changes in the last 500 years. On the other hand, most
402 of the dates used in this study are from the most superficial sediments of the megafan and they are
403 associated to volcanic sand sheets. Most of them mark the last massive sedimentation event linked to
404 lahars or hyperconcentrated floods in the sampled area. In this discussion we integrate dates with

405 geomorphic evidence to date the connection of the sampled area with volcanic source areas and the
406 abandonment of lobes as areas of active sedimentation.

407 The fluvial network of the Santa Clara Megafan appear to be impacted by two main periods of
408 major changes in recent times. The dates obtained in the eastern sector of the fan, fed by the Toro-
409 Amarillo River Basin, suggest there was a period of high sediment supply just at the beginning of our
410 era (*s.* I) that certainly disturbed the fluvial channels of this area. Sediment sampled in relation to
411 volcanic sand units in different points over the middle and distal zones show very similar ages,
412 implying a that lahars occurred frequently and cover an extensive area. From s. I to the present, the
413 available dating information point to a period with lower sedimentation in this sector, suggesting the
414 progressive abandonment of this part of the fan. The samples from the western sector of the fan, fed
415 by the Sucio River Basin, were collected strategically to know the evolution of the fluvial channels of
416 this area. From the obtained dates and the study of paleochannel evolution we deduced that this sector
417 was affected by great changes in last five centuries of our era (*s.* XV-XX). Between the *s.* I and *s.* XV,
418 it seems that there is an episode of ca. 1700 years of relative quiescence and minor changes in the
419 landscape of the eastern sector of the megafan where most of the samples in surficial deposits
420 associated to floods or lahars show ages older than two millennia (e.g. sample Mo-4 of a crevasse splay
421 deposit). We cannot argue that the western part of the megafan experienced this period of calm because
422 we sampled the surficial deposits that are younger than five centuries and we have not studied the
423 sediments below that could register lahar activity before that date. A very recent investigation on the
424 eruptions of Irazú (Alvarado et al., in prep.) seems to indicate that there are several eruptive periods
425 between s. I and s. XV that should have impacted the western area of the megafan (Figure 10).

426

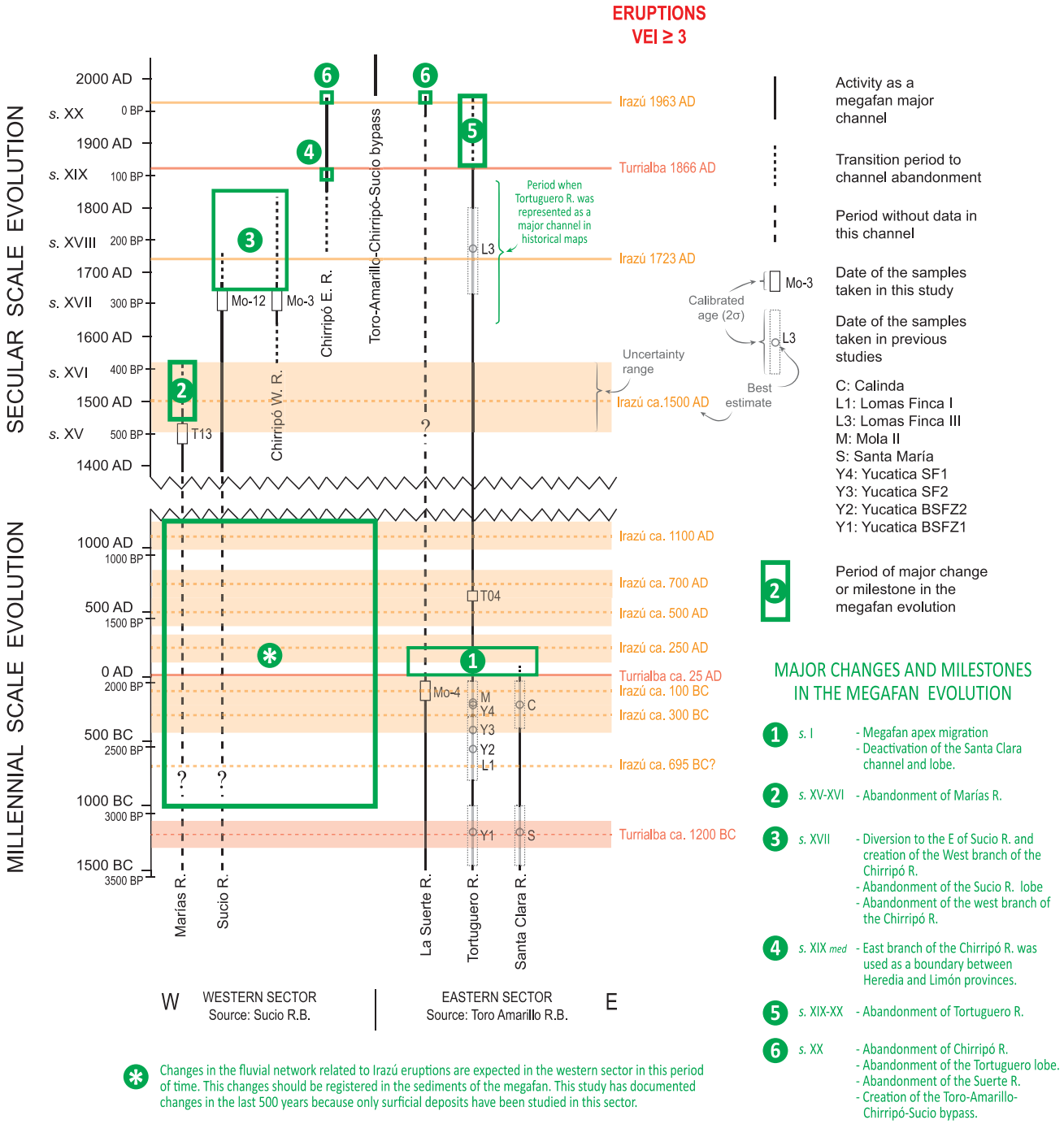

Figure 10. Diagram of the temporal and spatial distribution of the studied samples.

We found that changes in the megafan fluvial system can be associated to changes in the volcanic activity of the volcanoes in the region, which act as the headwater of the rivers. For example, the eastern sector of the megafan is influenced by the eruptions of the Turrialba Volcano, which is in the headwater of the Toro Amarillo River. The period of low sedimentation from *s.* I to *s.* XVIII in the

433 easter sector of the Santa Clara Megafan coincides with a period of low eruptive activity of the
434 Turrialba Volcano (Figure 10). Furthermore, the two periods when we recognize disturbance on fluvial
435 systems at *s.* I and *s.* XVIII in the eastern sector of the megafan are characterized by strong eruptions
436 (Figure 10).

437 If we go into detail, it seems that we have been able to register changes in the channels of the megafan
438 produced by eruptions with a Volcanic Explosivity Index (VEI) ≥ 3 (Figure 10). The last of these
439 strong eruptions, the 1963-65 AD eruption of Irazú, is responsible of the present-day configuration of
440 the Santa Clara Megafan because it triggered the major avulsion in the Chirripó River and the migration
441 to the west of the megafan's main channel (Figure 9). Taking as reference the later event, it is
442 reasonable to think that syn- and post- eruptive lahars associated to the ca. 1500 AD and 1723 AD
443 eruptions of Irazú (VEI=3) are behind (1) the abandonment of Marías River in the *s.* XVI and (2) the
444 creation of the Chirripó fluvial channel and the abandonment of the western sedimentation lobe of the
445 fan in the *s.* XVII, respectively. The strongest eruption of the Turrialba Volcano in the last millennia
446 that occurred in ca. 25 AD (Alvarado et al., in prep. and reference there in) is also correlated with sand
447 sheets studied by Dechesne (1994) and Van Ruitenbeek (1994). These authors dated clay deposits
448 directly underlying the sand sheets and obtained ages between *s.* IV B.C. and the first half of the *s.* I
449 B.C. (~2350-2000 B.P.) which constrain a maximum depositional age for the sand sheets. Therefore,
450 the overlaying sand sheets should be younger than this time range and they most likely are associated
451 to the great perturbation provoked by this strong eruption in the megafan source zone. The similar ages
452 obtained by Dechesne (1994) and Van Ruitenbeek (1994) in different locations along the eastern lobe
453 of the megafan certainly indicates a major sediment input event most likely associated to syn- and
454 post- eruptive period that covered most of the eastern sector of the megafan with volcanic sands in a
455 short period of time, probably decades (Figures 2 and 4).

Galve et al. (2016) invoked the tectonic activity as another driven force of the changes in the megafan. Our new results suggest that at timescales of years to millennia the role of tectonism in driving major avulsion events appear to be minor compared to the influence of eruptions. Earthquakes and other processes such as volcanic debris avalanches (triggered or not by eruptions or earthquakes) have been also involved in megafan changes but probably in a timely manner. Nevertheless, we are lacking a temporal catalogue of large landslides and paleo-earthquakes to confirm this statement.

5.2. Decadal, secular, and millennial evolution of the Santa Clara Megafan

In this section we connect our results, the findings of previous researches and the considerations provided in the previous section to describe the history of the Santa Clara Megafan during the last three millennia, from the recent times at decadal scale to those dates that thanks to dating methods, geomorphological interpretation and available outcrops have been achievable. In order to follow the description more easily, we have elaborated the Figure 11 where all the changes that we have recognized in the Santa Clara Megafan are reported. Figure 10 could be also of help to follow the narrative. In the following we focus on discussing the geomorphic changes that took place before the s. XX. We provide evidence that from s. I to s. XV the rate of geomorphic change in the eastern part of the Santa Clara Megafan was relatively low, whereas from s. XVI- s. XX there are important changes of the main active lobes of the megafan. We then link the rate of geomorphic change in the megafan to the frequency of volcanic eruptions occurring simultaneously.

First of all, we are going to describe the observed evolution in a decadal time scale. In that temporal scale, the tropical character of the main fluvial channels of the Santa Clara Megafan is clearly represented by their high dynamism (see e.g., Figure 6). Processes such as channels abandoning meanders occur in the matter of years and the rivers have ever-changing anabranching stretches. These rivers are not regulated and they are in a context of high precipitation that favor these rapid changes.

The decadal changes observed in the rivers of the Santa Clara Megafan occur over a spatial scale of nearly one kilometer wide in the proximal and medium sector of the megafan.

Also at a decadal scale, we observed that the fluvial channels at the apex of the proximal lobes of the megafan can undergo later channel migrations from one margin of the lobe to the other through river avulsions. First the water flow from the parent channel is diverted into the adjacent floodplain/basin as it bifurcates during avulsion. Subsequently, the sediment input from each lahar or flood event progressively fills the parent active channel as the sediment supply exceeds the reduced river's transport capacity. This process continues until the full abandonment and disconnection of the parent channel from the newly formed channel. A notable example event of decadal lateral channel migration was the progressive migration of Toro Amarillo River channel to the west (on the right side of Figure 8). This migration occurred at a progressive rate because channels were not abandoned abruptly but gradually. This migration produced a gradual disconnection of the Tortuguero and La Suerte rivers from its source area over the last 150-200 years and their definitive cut-off during the middle of *s.* XX (Figure 11F). The latter cut-off was accompanied by a total migration of the Toro Amarillo River from the eastern margin of its proximal lobe, abandoned before 1960, to the western margin, where the current channel has been established almost since 1985. Therefore, that river migrated laterally from one lobe margin to the other in less than 25 years significantly changing the megafan's depositional environment. We associate these abrupt changes to the syn- and post- eruptive laharic activity generated eruptions of the Irazú Volcano in the 1963-65 AD (Figure 11F).

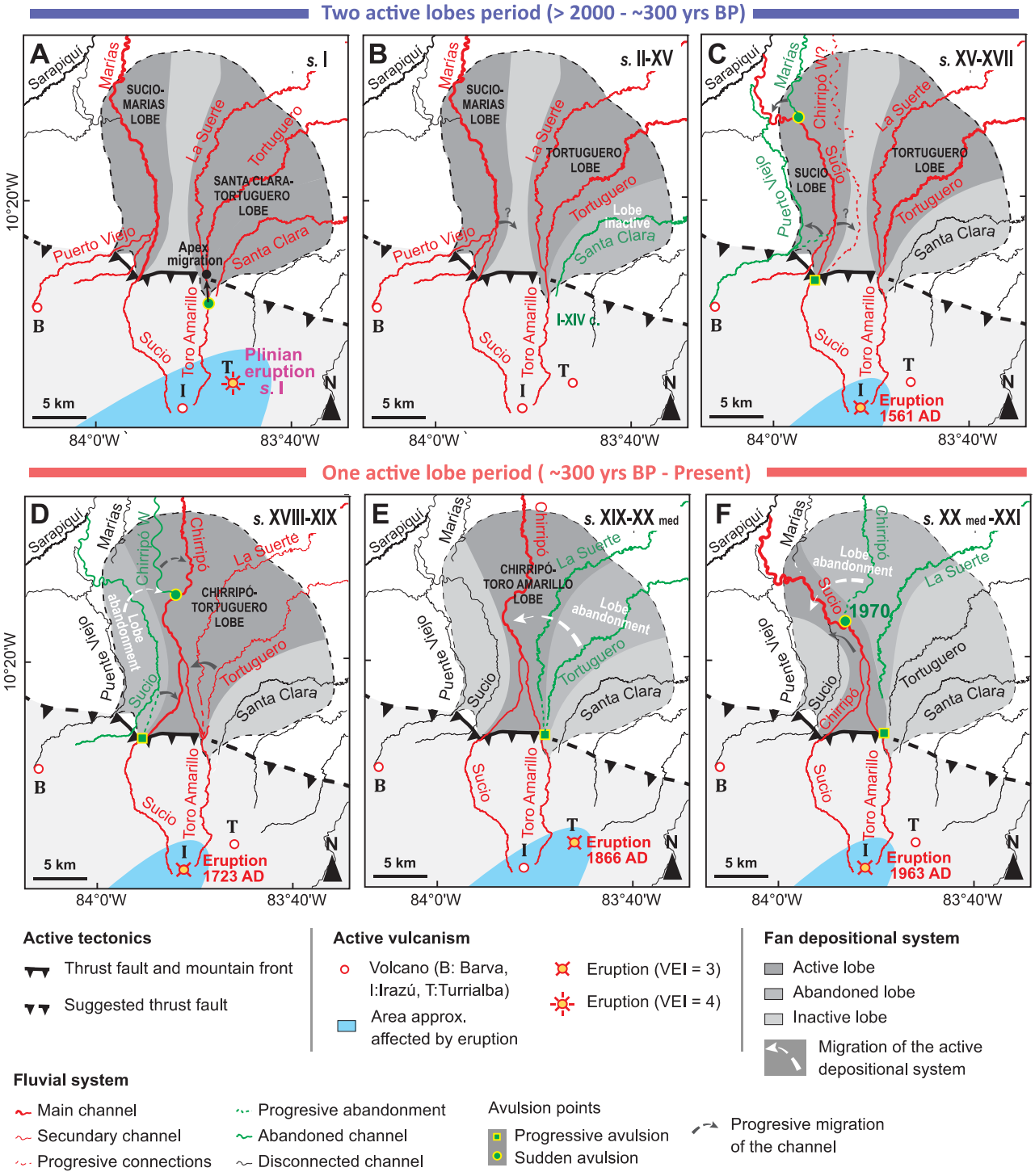

Figure 11. Schema of the evolution of the Santa Clara Megafan at the millennial, secular and decadal timescales

501 The most abrupt events that changed the megafan dynamics are those related to major avulsions
502 in the fluvial system that occur at nearly secular temporal scale. These major avulsions are sudden
503 changes in the trace of megafan's main channels that overcome the strip within which the river usually
504 migrates. These events produce river diversions of tens of kilometres and a great part of the river course
505 is totally abandoned within days. The last event of this type occurred in 1970 AD when the Chirripó
506 River was diverted towards the west, running into the Sucio River instead of continuing towards the
507 San Juan River located to the north (Figure 9; Nieuwenhuyse, 1996). Th diversion of the Chirripó
508 River was caused by a hyperconcentrated flood that deposited 6×10^6 to 24×10^6 m^3 of sand (Dechesne,
509 1994), overfilling the fluvial channel of Chirripó River in the area to the west of the village of San
510 Gerardo (Figure 9; Limón province). This event produced the abandonment of an entire depositional
511 lobe of the Santa Clara Megafan which used to be fed by the Chirripó River (Figure 11F).

512 Prior to 1970 AD, the paleo Chirripó River (green paleochannel in Figure 9) was formed from
513 the junction of the Sucio and Toro Amarillo rivers. Given that the river basins of the Sucio and Toro
514 Amarillo rivers occupy the total source area of the Santa Clara Megafan, the amount of sediment
515 transported and deposited by the paleo Chirripó River prior to 1970 AD must have been significant
516 and its westward diversion impacted the sedimentary dynamics of the megafan. In the present, the
517 Sucio-Toro Amarillo-Chirripó rivers converge into a single channel that conducts the sediments
518 directly to the Sarapiquí River and creates a bypass or barrier that prevents sediment delivery into the
519 Santa Clara Megafan (Figures 10 and 11F). This current situation appears to be quite unstable if we
520 take into account how dynamic the Santa Clara Megafan is. We presume that great geomorphic
521 changes in this river may occur in the future as a result of high sediment input from major lahars or
522 hyperconcentrated floods triggered by strong eruptions.

523 The evolution between s. XVIII to s. XX can be summarized in the confluence of Sucio and
524 Toro Amarillo rivers, resulting in the creation of the Chirripó River (Figure 11D, E, F). Chirripó River

acted as the main channel of the fan most probably from *s.* XVIII to the first half of *s.* XX. This hierarchy in the fluvial channels led to the gradual disconnection of the Tortuguero River and La Suerte rivers (Figure 11E). The abandonment of the Tortuguero River was especially significant as it used to be one of the megafan's main channels prior to s. XIX. The former relevance of the Tortuguero River can be recognized in the historical maps of the region from *s.* XVII to *s.* XIX that portray it (previously named as *Río de Vazquez)* as one of the main courses during the s. XIX. In contrast, the maps elaborated after the second half of *s.* XIX do not confer great importance to Tortuguero River (Table 1).

The course of the Chirripó River also experienced important changes before *s.* XX. A paleochannel dated with the sample Mo-3 suggests that a western branch of the Chirripó river was most likely active until the *s.* XVIII (Figure 9). From *s.* XVIII to *s.* XX_{med} the Chirripo River was the main course of the megafan. The establishment of the Chirripó River as the main course starts with the eastward migration of the paleo-Sucio River and the transformation of this river into the Chirripó River course (Figure 11C, D). The migration of the paleo-Sucio River involved two main avulsions: (1) the abandonment of the Marías River course (Figure 11C) and (2) the disconnection between the current course of actual Sucio River and the Sucio River headwaters (Figure 11D; see the present rivers with the same name in Figure 7). We estimate that those avulsions occurred in the *s.* XVI and the *s.* XVIII, respectively, according to the dates of the samples Mo-12 and T13 that constrain the maximum depositional age of the last great flood events in the paleochannels of these rivers. As mentioned in the previous section, we relate these avulsions with two strong eruptions in the Irazú Volcano that occurred in ca. 1500 AD and 1723 AD.

Between s. I to s. XV the megafan was configured by two main depositional lobes: the Sucio-Marias lobe and the Tortuguero lobe (Figure 10A-C). The Sucio-Marias lobe would have had its source area mainly in the headwaters of the modern Sucio River Basin and the Tortuguero lobe in the

549 headwaters of the modern Toro Amarillo River Basin. The only information about river dynamics in
550 the period from *s.* I to *s.* XV comes from geoarchaeological research carried out in the Nuevo Corinto
551 site (Figures 1 and 8) by Acevedo (2016). His data suggest that during the first centuries of our era
552 (The El Bosque period; *s.* III B.C. - *s.* III AD; Salgado et al., 2013) the Sucio River progressively
553 shifted westward. The westward migration of the Sucio River allowed the development of a human
554 settlement in the right bank of the river between 250 and 400 AD (Salgado et al., 2013).

555 From the descriptions on the fluvial deposits and geomorphology by Acevedo (2016) we infer
556 that at some point between *s.* IV and *s.* VIII (The Selva period; Salgado et al., 2013) the Sucio River
557 begin to migrate towards the east. The evidence from Acevedo (2016) is flooding in a sector of the
558 Nuevo Corinto site. This author does not provide additional evidence of flooding in this area in
559 subsequent periods. Nevertheless, the location of the active channel in the present and the
560 geomorphological evolution observed around the site (Figure 8) show clearly how the river have been
561 migrating towards the east in recent times (probably centuries) and it could be one of the reasons of
562 the abandonment of Nuevo Corinto in the *s.* XII (Acevedo, 2016).

563 Thus, we can deduce that the migration of the Sucio River from the west to the east margin of
564 its proximal lobe was much slower than the migration observed in the Toro Amarillo River during the
565 second half of the *s.* XX. We estimate that the Sucio River took from 9 to 13 centuries to shift its main
566 channel a total of 5 km (at a rate of 0.005-0.004 km/yr) from the margin that connected to the Sucio
567 and Marias River to the margin that connected to the Chirripó channel (Figure 11). In contrast, the
568 migration observed in the Toro Amarillo River during the second half of the *s.* XX occurred at a rate
569 of 0.16 km/yr. The slow diversion of Sucio River in its apex could be another reference of the low
570 pace of changes in the megafan in the period when strong eruptions were less frequent (*s.* I-XV).

571 We now focus in the *s.* I that is the beginning of the period of general quiescence in the eastern
572 sector of the megafan (*s.* I-XV). The *s.* I is marked by the strongest eruption in the region in the last

three millennia. This major event is the ca. 25 AD subplinian eruption of the Turrialba Volcano that we commented in the previous section. This episode, that we consider impacted the megafan for several decades, has two main effects (Figure 11A): (1) the abandonment of the eastern sector of the megafan crossed by the Santa Clara River and (2) the migration of the megafan apex to the north causing also de disconnection of the upper part of the megafan sedimentary body.

Before the disturbance produced by the Turrialba subplinian eruption in *s.* I, various high sedimentation events were registered as volcanic sand sheets deposited in the surroundings of the Tortuguero River (Dechesne, 1994; Van Ruitenbeek, 1994). In the Yucatica site, Van Ruitenbeek (1994) described and dated three sand sheets, two of them most likely separated by some centuries and the other probably separated by more than a millennium from the other two. This indicates two events of high sediment input most probably associated to the Turrialba subplinian eruption and the Irazú eruption of the *s.* VII B.C., preceded by a period of quiescence, which in turn is preceded by another event of high sediment supply that we associate to the ca. 1200 B.C. eruption of Turrialba. This succession shows a similar temporal pattern than that of the one observed during our era: After a great event of sediment supply comes a quiescence period, which in turn it is followed by another period of major changes and high sediment input in the megafan, all mostly correlated with volcanic activity.

In this sense, it is an open question if there is a cyclical character in the megafan evolution and volcanism at millennial scale with a quiescence period of about a millennia or more followed by some centuries of high activity that finish in a major eruption that strongly disrupt the megafan's environment again.

5.3. Additional findings from the study of the megafan evolution

Our study offers other useful findings to better understand the rates of erosion and sedimentation in the megafan. This information supports the previous estimations in the region on these parameters and it could be useful for future research on landscape evolution. On one hand, the sample Mo-5 dates

sediments included in a so-called “red hill” (Figure 3F). This term was used by the Dutch researchers (van Seeters, 1993; Dechesne, 1994; van Ruitenbeek, 1994 and Niewenhuyse, 1996) to describe bodies of dissected terraces or isolated hills of up to 10 m high observed in the megafan. These authors assigned a Pleistocene age to that hills (van Ruitenbeek, 1994) and our sample indicates that the age of the materials that forms the sampled hill were deposited less than 5,000 years ago. A question that remains open is the precise age of the erosion event that formed the red hills and the mechanism that triggered the event.

We also calculated an incision rate in the megafan apex of ~6 m/ka in the sample site of T06 considering a total fluvial incision in this point of 15 m since 2400 years ago (Figure 8). This value is higher than the rate estimated by Kesel and Lowe (1986), 3.8 m/ka, but in the same order of magnitude. Furthermore, these rates are also in the same order of magnitude of the incision rates previously estimated by Galve et al. (2016) at catchment scale.

On the other hand, we estimated sedimentation rates of ~1 m/ka in the apex area of the megafan using the dating of our samples T06 (ca. 2400 BP) and Mo-14 (ca. 17200 BP) and the stratigraphic thickness of 15 m that separates these samples (Figure 8). Our sedimentation rate value is in accordance with those roughly estimated by Galve et al. (2016) who infer rates > 0.6 m/ka as average sedimentation rates for the Santa Clara Megafan. We also estimated the sedimentation rate in the Yucatica site (Figure 4J) as ~1 m/ka using the data from van Ruitenbeek (1994) (up to 3 m of sediments in almost 3 ka).

5.4. Implications for archeological and historical studies

In the same way that geomorphological studies such as ours took advantage of archeological findings (see section 5.2) several archaeological studies have benefited from geological and geomorphological investigations of alluvial environments. Great example interdisciplinary studies are the works of Heyvaert et al. (2012, 2016) and Jotheri et al. (2016, 2018) who integrated

621 geomorphological, sedimentological, archeological and historical information to analyze avulsions in
622 the Lower Khuzestan (Iran) and Mesopotamia (Iraq). Another remarkable example of interdisciplinary
623 work is the paper of Singh et al. (2017) where they use pure geological techniques to change a
624 paradigm that explained the distribution of the Bronze-age Indus Civilization settlements (~4.6–3.9 ka
625 BP).

626 The evolution of the fluvial system described in this paper can be of great help to understand
627 the landscape of the Santa Clara lowlands during the human occupation of the region from 1000 BC
628 to present. Archaeologists and historians may use this information to define strategies for their
629 prospection surveys or to support their work hypothesis in a region with a changing landscape and
630 little known from the archaeological and historical point of view. In this sense, the new data gathered
631 during our investigation was already helpful for the interpretations of Alvarado et al. (in prep.)
632 regarding the historical eruptions of s. XIX in the Turrialba volcano.

633 Furthermore, there is ongoing research in the region about a road used since pre-Colombian times that
634 connect the El Valle Central of Costa Rica with the mouth of the San Juan River and the Tortuguero
635 and Mosquito coasts (Salgado et al., 2016). This road was an important commercial route from *s.* IV
636 to *s.* XII connecting the Santa Clara region with as far afield as Mexico or Colombia (Salgado et al.,
637 2016 and references there in). Several pre-Colombian settlements have been discovered along this
638 road. During the Spanish colonization this road was used as smuggling route and for military proposes
639 to control incursions from the north by English troops and/or Mosquitians (Salgado et al., 2016). The
640 route was later forgotten until the archaeological studies of the last decade brought to light the stretch
641 of the road from the El Valle Central to the archaeological sites of Nuevo Corinto, Las Flores, and La
642 Manuda in the Santa Clara plain, at the foot of the Irazú volcano (Figures 1 and 8) (Cavallini, 2011;
643 Salgado et al., 2016). The new paleogeographical reconstructions (Figure 11) derived from this
644 research on the Santa Clara Megafan can contribute to clarify which route was used between the cited

sites and the Tortuguero and Mosquito coasts and new archaeological sites may be found in the process.

5.5. Implications for volcanic risk assessments

Our new findings support the observations already pointed out by Galve et al. (2016) about the lahar (debris flows and hyperconcentrated floods) hazards in the Santa Clara lowlands. They indicate that this region is exposed to "syneruptive, posteruptive and co-seismic lahars" and other torrential processes, "which can abruptly change the landscape of the megafan" (Galve et al., 2016). The new data presented in this paper indicates that the link between volcanic eruptions and these hydrologic phenomena. When eruptions of VEI $\geq$ 3 occur the hazard of great changes in the megafan fluvial system is high and a major avulsion event is very likely. Moreover, our results reveal that eruption-, earthquake- or landslide-related lahars can reach areas at more than 50 km from the source (see avulsion points in Figure 11). The long distance reached by some of this volcanic derived sediment fluxes is somewhat reminiscent of tragic cases such as the 1985 Armero (Colombia) disaster (Lowe et al., 1986). We underscore the high risk of disaster that these volcanic events pose to communities living in the Santa Clara Megafan. This risk has not been adequately taken into account in the last lahar hazard analysis carried out in the region (Ruiz et al., 2015) and we suggest that their lahar run-out estimations must be revised.

Regarding volcanic hazards in Costa Rica, there is a major unresolved question: Is there a constant cycle of volcanic activity with a periodicity in the Irazú and Turrialba volcanoes? If so, are we near the end of a period with increased activity and we must expect a strong eruption in the following decades or in the next century?

The amount of existing chronological data in the Santa Clara Megafan is not enough to answer these questions definitively, thus further chronological studies are required in the volcanic rocks that cover the slopes of the volcanoes and in the sediments of the megafan where the great eruptions and

669 other important events eventually result in sediment deposition. There are examples of chronological
670 studies that can be used as a base, including the one of Procter et al. (2009) in the Mt Taranaki (New
671 Zealand) who extract information of the volcano evolution from the sediments of its ring plain and the
672 one of Pardo et al. (2019) which carried extensive field mapping and geochronology of volcanic
673 sequences in the tropical Andes of Colombia.

674 In the case of the Santa Clara Megafan, there are great challenges of carrying chronological studies
675 due to the absence of good outcrops in the Santa Clara plain which makes it difficult to measure
676 stratigraphic columns and collect samples on a long stratigraphic interval. However, one possibility to
677 overcome the lack of outcrops is to develop a borehole drilling survey and an exhaustive analysis of
678 the boreholes stratigraphy and sediments combining different techniques as is done in
679 paleoclimatology studies. Studying data from several boreholes may reveal the cyclicity of great
680 eruptions in the region and thus help to predict if a strong eruption is likely in the future. All these
681 scientific efforts must be combined with prevention to increase the resilience of the Costa Rican society
682 against a damaging future event.

683 **5.6. Santa Clara Megafan recent evolution and other non-volcanogenic megafans**

684 The Santa Clara Megafan has is special compared to other megafans at it has been developed
685 in a tropical rainforest climate at 23.5°N-23.5°S of latitude where megafans are not so common (see
686 databases of Leier et al., 2005, Hartley et al., 2010 and Weismann et al., 2010) except for cases such
687 as the tropical Cauca/Magdalena (Weismann et al., 2015; Perez-Consuegra et al., 2021) or Pastaza
688 (Bernal et al., 2011) megafans. The most iconic modern megafans (e.g., Kosi, Taquari, Okavango,
689 Chaco plain megafans) are in regions with subtropical climates between 20° and 35° N and S latitude.
690 Leier et al. (2005) analyzed a dataset of megafans around the world and determined that rivers in these
691 regions the precipitation patterns are highly seasonal which results in rivers having large fluctuations
692 in discharge.

693 The high discharge variability of the sub-tropical rivers is thought to enhance the erosion in
694 watersheds, which increases the sediment supply and aggradation rate in the receiving basins, and, if
695 certain conditions are met (e.g., basin accommodation space, spacing between channel outlets), a
696 megafan or fluvial fan is formed (Leier et al., 2005; Hartley et al, 2010). Hartley et al. (2010) expanded
697 the megafan database (using the term Distributive Fluvial System to refer to megafans) and revised
698 the relationship between megafan occurrence and climatic setting, latitudinal location and geological
699 context, pointing out that megafans may form at different climatic and geological settings around the
700 world and they are not indicators of a precise climate. Recently, Hansford and Plink-Björklund (2020)
701 analyzing discharge data of a global database of rivers that generate fluvial fans and megafans
702 concluded that these large fans are produced by rivers in settings that promote avulsions and with
703 modern high discharge variability or high variability under past climate regimes. Most of the analyzed
704 rivers (75%) show present-day high discharge variability and those with current moderate-low
705 discharge variability could have had high fluctuations in the past under climate regimes different from
706 current one (e.g., the Chaco fans, Latrubesse et al., 2012; the southern alpine fans, Fontana et al.,
707 2014b; or the Taquari fan, Assine and Soares 2004).

708 In general, tropical rivers such as those draining into the Costarrican Caribbean lowlands do
709 not show high fluctuations in discharge compared to rivers with high discharge variability in higher
710 latitudes (e.g., Hansford et al., 2020). For example, in the Sarapaqui River there is high precipitations
711 throughout the year and the differences between the “dry” and “humid” seasons are not very
712 significant. The Sarapaqui River (drainage area 821 km^2) has an average monthly discharge of ~150
713 m^3/s in the two wet seasons (August and December; Figure S1; Global Runoff Data Centre) and of
714 75–90 m3/s on the driest seasons (April and September). This two-fold variation in average monthly
715 discharge is not very large. In a decadal or secular climate timescale, hurricanes should be considered.
716 Caribbean hurricanes can produce high discharge peaks in the area and produce high daily discharge
717 variability but they usually impact Costa Rica indirectly and, for example, none of these has arrived to

718 mainland Costa Rica during *s.* XX (Alfaro and Pérez-Briceño 2014). Hurricane Otto in November
719 2016 was the first hurricane that made a landfall in northern Costa Rica since records have been kept
720 (Quesada-Román et al., 2019).

721 Besides high discharge variability other factors such as deforestation can enhance erosion in
722 the upland source area and increase the sediment supply into the lowlands promoting avulsions (Bernal
723 et al., 2011). An extreme example are the historical human-induced avulsions in the Yellow River
724 fluvial fan (China) triggered by large-scale deforestation in the middle section of the river basin during
725 the Middle Ages (Chen, 2019). High economic development provoked the deforestation that caused
726 an extreme increase of erosion in the Loess Plateau transforming the Yellow river in a sediment-laden
727 river with a high aggradation capacity. Later a convulsive war period caused a lack on the management
728 of the Yellow river and the frequency of avulsions increased artificially as high as once every 20 years
729 (Chen, 2019).

730 The avulsion rate in the Santa Clara Megafan is lower than the one estimated for the Yellow
731 River in the Middle Ages, but this case is illustrative to contrast the processes that may controlling
732 high sediment yields in the Santa Clara Megafan. The great vegetation cover supported by the tropical
733 rainforest climate mainly limits the erosion processes in the Santa Clara Megafan's source area. In
734 contrast to cases as the Yellow River where the large sediment supply events needed to provoke
735 avulsions and aggradation generated by perturbations due to human activities or due to climate, in the
736 Santa Clara Megafan the perturbations are mainly related to volcanic eruptions. As mentioned in the
737 previous section, volcanic eruptions produce these perturbations (Galve et al., 2016) during a syn- and
738 post- eruptive periods. The volcanic ash falls during eruptions trigger changes in the hydrological and
739 sedimentary-yield of the rivers (Manville et al., 2009; Pierson et al., 2014), because they generate
740 deforestation in the catchments. The ash falls kills the vegetation favouring locally the erosion
741 processes. In addition, the volcanic deposits (e.g., ash and pyroclasts) that are deposited during the

742 eruption and cover the surface of the volcano surroundings have high erodibilities and thus can easily
743 increase the sediment yield of the rivers when they are mobilized during rainfall events.

744 The magnitude of the eruption and the characteristics of the impacted region determine the
745 duration of this eruption response period (Manville et al., 2009; Pierson et al., 2014), which in the case
746 of the studied megafan, may cover from months to years. For example a historical eruption such as it
747 was observed in the Irazú Volcano eruption in 1963-65 caused a major avulsion in the Chirripó River
748 (Figure 11F) five years later (1970). However, it cannot be ruled out that there were longer eruption
749 response periods (i.e., decades) for the pre-historical sub-subplinian or subplinian eruptions of the
750 Turrialba Volcano. Furthermore, these syn- and post- eruptive periods, when the Santa Clara Megafan
751 is disrupted by strong eruptions, are separated by inter-eruptive periods when we observed little
752 changes in the megafan landscape (e.g. *s.* II-XV period).

753 The avulsion rate in the Santa Clara Megafan for the past five centuries is ~1 major
754 avulsion/century. The last five centuries is the period when we have the better control on the megafan
755 changes (three sudden avulsions and two progressive shifts and abandonment of channels, Figures 10
756 and 11). The rate of eruptions with VEI $\geq$ 3 during the last five centuries in the source area was 0.8
757 eruptions/century, a value close to the avulsion rate.

758 The rate of fluvial changes in the Santa Clara Megafan is slow in comparison with the evolution
759 of megafans driven by intense wet-season monsoon precipitation such as the Kosi Megafan. In the
760 Kosi Megafan the channels migrated from one margin of the fan to the other (~100 km) in just 164
761 years (migration velocity: 0.6 km/yr; Chakraborty et al., 2010). In contrast, in the Santa Clara Megafan
762 the margin-to-margin migration of channels was much slower, lasting about two millennia. The
763 difference in the rates of channel migration is even more substantial when considering that the Kosi
764 Megafan is two times wider than the Santa Clara Megafan (~50 km; migration velocity: ~0.02 km/yr).
765 Regarding avulsion rates, the Santa Clara Megafan (~1 avulsions/century) has lower rates than the rate

766 estimated for the Kosi Megafan (4.8 avulsions/century). Similar avulsion rates to that of the Kosi
767 Megafan have been observed in megafans impacted by human activities in their source areas such as
768 the Taquari (6.7–10 avulsions/century) and the Yellow River (~5 avulsions/century) fluvial fans
769 (Assine and Soares 2004; Zani et al., 2012; Chen, 2019).

770 There are at least two examples of megafans with avulsion rates similar to the rate estimated in
771 the Santa Clara Megafan. One of them is the Okavango Megafan (Botswana) that has been impacted
772 by three major avulsions in the last two centuries (1.5 avulsions/century) (Bean, 2018). This megafan
773 is in a semi-arid climate, with moderate discharge variability (Hansford and Plink-Björklund, 2020)
774 and the causes of its avulsions are unclear so far. Bean (2018) invokes a combination of anthropogenic,
775 zoogenic, tectonic and climatic causes that trigger avulsions in the Okavango River. Therefore, the
776 Okavango is a complex setting difficult to compare with the Santa Clara case. Another case is the
777 Pastaza Megafan (Perú-Ecuador), which is not a conventional megafan. It is in a similar tropical
778 climate as the Santa Clara Megafan, in the eastern piedmont of the Northern Andes and is part of the
779 Amazonian Basin. Bernal et al. (2011) estimated a rate of 0.51 avulsions/century for the last 20 ka in
780 the Pastaza Megafan.

781 The rate of avulsions in the Pastaza Megafan is in the same order of magnitude as the rate of the Santa
782 Clara Megafan and may be more similar if we would have considered a long-term rate in the latter
783 taking into consideration the low activity period from *s.* II to *s.* XV. The rates of avulsion of the tropical
784 Pastaza and Santa Clara Megafans are one order of magnitude below those of the monsoonal or human-
785 impacted megafans but greater than rates estimated in major rivers not associated to megafans such as
786 the Saskatchewan River (Canada) that cross a region with cold continental climate with low
787 precipitation (0.17 avulsions/century, Morozova and Smith, 2000) or the Po River (Italy) that cross a
788 region with a mild continental and a humid subtropical climates (0.25 avulsions/century, Nelson 1970
789 in Mackey and Bridge 1995).

Similar to the Santa Clara Megan, the source area of the Pastaza Megafan is also impacted by active volcanism and its apex is located on the eastern boundary of sub-Andean active tectonic structures. Previous studies did not consider the role of vulcanism in the Pastaza Megafan (Bernal et al., 2011). However, we observe many similarities between both megafans and suggest that the genetic model of the Santa Clara Megafan from this study and that of Galve et al. (2016) could probably be applied to the Pastaza Megafan.

We can conclude from the geomorphic observations and the chronology data that the formation of the Santa Clara Megafan is connected to cyclical high sediment load events. The cycles of these events are linked with the cycles of the processes that generate the events. In the other detailed studied megafans, seasonal (i.e., moonson), inter-annual (i.e. El Niño) or even decadal, secular or millennial climate processes (i.e. heating or cooling/glacial and inter-glacial periods) commonly determine this kind of cyclical events. When climate is relatively constant through long periods of time and it do not show a great cyclical variability as in the equatorial regions with rainforest tropical climates (Hansford et al., 2020), another driving force must be invoked to explain megafan formation. We have pointed out how humans through deforestation can also trigger aggradation events in modern megafans following socio-economic cycles. However, the influence of humans on the landscape is too short (i.e., millennia) to explain the megafan formation that can be extended for hundreds of millennia. As previous authors and we have stated (van Seeters, 1993; Dechesne, 1994; van Ruitenbeek, 1994 and Niewenhuyse, 1996; Galve et al., 2016), volcanic eruptions are the alternative processes required to explain the formation of the Santa Clara Megafan. It is a good example of how eruptions can generate the high sediment transport and deposition events behind the formation of a megafan in equatorial settings. Eruptions are often cyclical endogenous processes (e.g. Michaut et al., 2013) that provide new material to the Earth surface prone to be easily eroded during the syn- and post- eruption periods (Manville et al., 2009; Pierson et al., 2014). In the humid tropics, lahars fed fans and megafans in a

814 cyclical pace associated to that of the active volcanism. As we have shown, changes and activity in the
815 Santa Clara Megafan will be determined by these volcanic cycles, almost at centennial temporal scale.

816 **6. Conclusions**

817 We assembled a detailed description of the evolution of the Santa Clara Megafan during the last three
818 millennia using different approaches: remote sensing analysis, geomorphological investigations,
819 revision of historical documents and analysis of ancient maps, sedimentological assessment and dating
820 of fan deposits. The inferred evolution is temporally and spatially correlated with volcanic activity and
821 proves the influence of volcanic phenomena on the megafan fluvial dynamics. We observed how great
822 changes in the megafan channel configuration during the last five centuries are correlated in time with
823 periods of intense volcanic activity. In contrast, a period of less volcanic activity in the Turrialba that
824 lasted from *s.* I to *s.* XIX coincide with fewer changes in the eastern megafan's environment. We
825 detected that eruptions with a VEI ≥ 3 have the capacity to greatly change the fluvial system of the
826 megafan as in the cases of the Irazú Volcano eruptions of 1963-65 AD, 1723-24 AD and ca. 1500 AD,
827 and in the Turrialba eruption of *s.* I. These major changes together with other minor shifts produced a
828 specific dynamism in the megafan characterized by confluence and migrations of active lobes at a
829 secular pace. Thus, we registered how the main sedimentation activity in the megafan migrated from
830 the eastern sector to the western one in about two millennia. This migration has been developed
831 progressively in some parts of the megafan such as in the proximal lobes and episodically with abrupt
832 changes driven by volcanic-related processes through avulsions in the major fluvial channels.

833 Our paleogeographical reconstructions have the potential to guide future archeological research in the
834 studied region. Furthermore, the estimated avulsion rates show that society should consider lahars and
835 river diversion phenomena to increase its resilience against these hazardous processes associated to
836 the megafan formation and evolution. In this sense, the megafan sediments can also be used as a source
837 of information about volcanic activity in the region and provide inputs for volcanic risk assessments.

On the other hand, we concluded that the avulsion rate in the Santa Clara Megafan is different from other well-known non-volcanogenic megafans and it is mostly determined by the eruption frequency. The example provided by the Santa Clara Megafan show how the formation of megafans is linked to cyclical high sediment input events and the cycles of these events are connected to the cyclicity of exogenous or endogenous processes that control them.

Acknowledgements

This research was funded by very different sources. The work of J.P.G., P.R., J.V.P.-P. and J.M.A. was supported by the "Ramón y Cajal" Programme (RYC-2017-23335) of the Spanish Ministry of Science, the project "MORPHOMED"-PID2019-107138RB-I00/SRA (State Research Agency/10.13039/501100011033) and the project "RADANDALUS" (P18-RT-3632), and B-RNM-305-UGR1818 of the FEDER/Junta de Andalucía-Consejería de Transformación Económica, Industria, Conocimiento y Universidades. N. Pérez-Consuegra was funded by the MIT-Molina Postdoctoral Fellowship. The samples' dating was carried out with the financial support of the company "Falck Group" (Italy) and the "Ramón y Cajal" Grant (RYC-2017-23335). We thank the Instituto Costaricense de Electricidad (ICE) and the Centro de Nacional de Emergencias de Costa Rica (CNE) for making available essential data for this research and for the necessary means used in our field surveys in Costa Rica. The field campaigns were also financed by the Grant programme of the Banco Santander 2016. Shuttle Radar Topography Mission (SRTM) 1 Arc-Second Global and Landsat images are available from the U.S. Geological Survey; aerial photographs and topographic maps of the study area are available from the Instituto Geográfico Nacional de Costa Rica (IGN); and Sentinel 2 images are available from European Union's Copernicus Programme. We thank webs, on-line catalogues and libraries that make available historical maps.

References

862 Acevedo, B., 2016. Análisis geoarqueológico de los cambios ambientales y la ocupación de espacios,
863 dentro del sitio arqueológico Nuevo Corinto (1500 a.C. – 1550 d.C.), Limón, Costa Rica.
864 Universidad de Costa Rica.

865 Alfaro, E.J., Pérez-Briceño, P.M., 2014. Análisis del impacto de fenómenos meteorológicos en Costa
866 Rica, América Central, originados en los mares circundantes. Revista de Climatología 14, 1–11.

867 Alvarado, G., Mora, M., Ulloa, A., 2013. La Caída De "Ceniza" Proveniente Del Volcan Irazú (Costa
868 Rica) El 8 De Diciembre De 1994: ¿Una Explosión Freática? Revista Geológica de America
869 Central 48, 159–168.

870 Alvarado, G.E., Campos, D., Brenes-André, J., Alpizar, Y., Nuñez, S., Sojo, D., Esquivel, L., 2021.
871 Peligro Volcánico del Irazú, Costa Rica. Comisión Nacional de Prevención de Riesgos y Atención
872 de Emergencias (CNE) de Costa Rica.

873 Alvarado, G.E., Carr, M.J., Turrin, B.D., Swisher, C.C., Schmincke, H.-U., Hudnut, K.W., 2006.
874 Recent volcanic history of Irazú volcano, Costa Rica: Alternation and mixing of two magma
875 batches, and pervasive mixing. Geological Society of America Special Papers 412 , 259–276.

876 Alvarado, G.E., Esquivel, L., Sánchez, B.E., Matamoros, G., 2020. Peligro Volcánico del Turrialba,
877 Costa Rica. Comisión Nacional de Prevención de Riesgos y Atención de Emergencias (CNE) de
878 Costa Rica.

879 Alvarado, G.E., Esquivel, L., Sánchez, B.E., Matamoros, G., in prep. Peligro Volcánico del Irazú,
880 Costa Rica. Comisión Nacional de Prevención de Riesgos y Atención de Emergencias (CNE) de
881 Costa Rica.

882 Alvarado, G.E., Vega, A.E., 2011. La geomorfología de la colada de Cervantes, volcán Irazú (Costa
883 Rica): Descripción de uno de los campos de lava más grandes de América Central. Rev. geol. Am.
884 cent. https://doi.org/10.15517/rgac.v0i48.12238

885 Assine, M.L., Soares, P.C., 2004. Quaternary of the Pantanal, west-central Brazil. Quat. Int. 114, 23–
886 34.

887 Baker, V.R., Hamilton, C.W., Burr, D.M., Gulick, V.C., Komatsu, G., Luo, W., Rice, J.W., Jr,
888 Rodriguez, J.A.P., 2015. Fluvial geomorphology on Earth-like planetary surfaces: A review.
889 Geomorphology 245, 149–182.

890 Bean, R.A., 2018. Hydro-geomorphic dynamics in the Makgadikgadi Okavango Zambezi Basin,
891 Northern Botswana. University of Texas at Austin. https://doi.org/10.15781/T23776G2S

892 Bernal, C., Christophoul, F., Darrozes, J., Soula, J.C., Baby, P., Burgos, J., 2011. Late Glacial and
893 Holocene avulsions of the Rio Pastaza Megafan (Ecuador-Peru): Frequency and controlling
894 factors. Int. J. Earth Sci. 100, 1759–1782.

895 Brandes, C., Astorga, A., Littke, R., Winsemann, J., 2008. Basin modelling of the Limón Back-arc
896 Basin (Costa Rica): Burial history and temperature evolution of an island arc-related basin-system.
897 Basin Res. 20, 119–142.

898 Cavallini, C., 2011. El camino precolombino del Sitio Arqueológico Alto del Cardal C-304 AC.
899 Cuadernos de Antropología 21, 1–8.

900 Chakraborty, T., Kar, R., Ghosh, P., Basu, S., 2010. Kosi megafan: Historical records, geomorphology
901 and the recent avulsion of the Kosi River. Quat. Int. 227, 143–160.

902 Chen, Y., 2019. Flood dynamics of the lower Yellow River over the last 3000 years: Characteristics
903 and implications for geoarchaeology. Quat. Int. 521, 147–157.

De Souza, O.C. a. c., Araujo, M.R. a. c., Mertes, L.A.K. b. d., Melack, J.M. b. e., 2002. Form and process along the Taquari River alluvial fan, Pantanal, Brazil. Z. Geomorphol. Suppl. 129, 73–107.

DeCelles, P.G., Cavazza, W., 1999. A comparison of fluvial megafans in the Cordilleran (Upper Cretaceous) and modern Himalayan foreland basin systems. Bulletin of the Geological Society of America 111, 1315–1334.

Dechesne, M., 1994. Island-arc volcanism and episodic fluvial sedimentation in the Atlantic Zone of Costa Rica. CATIE/AUW/MAG. Atlantic Zone Programme. Report No. 91. Field Report No. 137. Costa Rica. sp.

Fallas, M., Prado, A., Mora, M.M., Ruiz, P., Alfaro, E.J., Soto, G.J., 2018. El deslizamiento del 8 de diciembre de 1994 en el Volcán Irazú (Costa Rica): aspectos históricos y geomorfología con base en fotografías aéreas históricas y recientes. Revista Geológica de América Cental 58, 55–84.

Fontana, A., Monegato, G., Zavagno, E, Devoto, S., Burla, I., Cucchi, F., 2014a. Evolution of an Alpine fluvioglacial system at the LGM decay: The Cormor megafan (NE Italy). Geomorphology 204, 136–153.

Fontana, A., Mozzi, P., Marchetti, M., 2014b. Alluvial fans and megafans along the southern side of the Alps. Sediment. Geol. 301, 150–171.

Frantzius, A. von, 1861. Originalkarte des nördlichen Theiles von Costarica, nach einer Original-Zeichnung.

Galve, J.P., Alvarado, G.E., Pérez-Peña, J.V., Mora, M.M., Booth-Rea, G., Azañón, J.M., 2016. Megafan formation driven by explosive volcanism and active tectonic processes in a humid tropical environment. Terra Nova 28, 427–433.

925 Gohain, K., Parkash, B., 1990. Morphology of the Kosi megafan. In: A.H Rachocki, M Church (Eds.),
926 Alluvial Fans: a Field Approach, Wiley, Chichester (1990), pp. 151-178.

927 Hansford, M.R., Plink-Björklund, P., 2020. River discharge variability as the link between climate and
928 fluvial fan formation. Geology 48, 952–956.

929 Hansford, M.R., Plink-Björklund, P., Jones, E.R., 2020. Global quantitative analyses of river discharge
930 variability and hydrograph shape with respect to climate types. Earth-Sci. Rev 200, 102977.

931 Hartley, A.J., Weissmann, G.S., Nichols, G.J., Warwick, G.L., 2010. Large Distributive Fluvial
932 Systems: Characteristics, Distribution, and Controls on Development. J. Sediment. Res. 80, 167–
933 183.

934 Heyvaert, V.M.A., Walstra, J., 2016. The role of long-term human impact on avulsion and fan
935 development. Earth Surf. Processes Landforms 41, 2137–2152.

936 Heyvaert, V.M.A., Walstra, J., Verkinderen, P., Weerts, H.J.T., Ooghe, B., 2012. The role of human
937 interference on the channel shifting of the Karkheh River in the Lower Khuzestan plain
938 (Mesopotamia, SW Iran). Quat. Int. 251, 52–63.

939 Hidalgo, P.J., Alvarado, G.E., Linkimer, L., 2004. La Lavina Del Valle Central (Costa Rica): ¿Lahar
940 O Debris Avalanche? Revista Geológica de América Central 30, 101–109.

941 Horton, B.K., Decelles, P.G., 2001. Modern and ancient fuvial megafans in the foreland basin system
942 of the central Andes , southern Bolivia : Implications for drainage network evolution in fold- thrust
943 belts. Basin Res. 13, 43–63.

944 Instituto Costarricense de Electricidad (ICE)., 2016. Meteorological database from the “Area de
945 Hidrología”. [Database]. C.S. Estudios Básicos de Ingeniería: Pronóstico, Procesamiento y
946 Análisis Meteorologico, Área de Hidrología. San José, Costa Rica (Retrieved 23 February 2016).

947 Jotheri, J., Allen, M.B., Wilkinson, T.J., 2016. Holocene avulsions of the Euphrates river in the najaf
948 area of western Mesopotamia: Impacts on human settlement patterns. Geoarchaeology 31, 175–
949 193.

950 Jotheri, J., Altaweel, M., Tuji, A., Anma, R., Pennington, B., Rost, S., Watanabe, C., 2018. Holocene
951 fluvial and anthropogenic processes in the region of Uruk in southern Mesopotamia. Quat. Int. 483,
952 57–69.

953 Kesel, R.H., Lowe, D.R., 1987. Geomorphology and Sedimentology of the Toro Amarillo Alluvial
954 Fan in a Humid Tropical Environment, Costa Rica. Geogr. Ann. 69, 85–99.

955 Latrubesse, E.M., 2015. Large rivers, megafans and other Quaternary avulsive fluvial systems: A
956 potential "who's who" in the geological record. Earth-Sci. Rev. 146, 1–30.

957 Leier, A.L., DeCelles, P.G., Pelletier, J.D., 2005. Mountains, monsoons, and megafans. Geology 33,
958 289–292.

959 Lowe, D.R., Williams, S.N., Leigh, H., Connort, C.B., Gemmell, J.B., Stoiber, R.E., 1986. Lahars
960 initiated by the 13 November 1985 eruption of Nevado del Ruiz, Colombia. Nature 324, 51–53.

961 Manville, V., Németh, K., Kano, K., 2009. Source to sink: A review of three decades of progress in
962 the understanding of volcaniclastic processes, deposits, and hazards. Sediment. Geol. 220, 136–
963 161.

964 Mende, A., 2001. Sedimente und Architektur des Forearc-und Backarc-Becken von Südost-Costa Rica
965 und Nordwest-Panamá. Inst. f. Geologie u. Paläontologie.

966 Michaut, C., Ricard, Y., Bercovici, D., & Sparks, R. S. J. (2013). Eruption cyclicity at silicic volcanoes
967 potentially caused by magmatic gas waves. Nature Geoscience, 6(10), 856–860.

968 Moore, J.M., 2005. Large alluvial fans on Mars. J. Geophys. Res. 110.
969 https://doi.org/10.1029/2004je002352

970 Morozova, G.S., Smith, N.D., 2000. Holocene avulsion styles and sedimentation patterns of the
971 Saskatchewan River, Cumberland Marshes, Canada. Sediment. Geol. 130, 81–105.

972 Muller, C., Pacheco, J., Angarita, M., Alvarado, G., Sánchez, B., Avard, G., 2020. El deslizamiento
973 de las Torres del Irazú del 2020 (Costa Rica): antecedentes, colapso y situación actual.

974 Nelson, B.W., 1970. Hydrography, sediment dispersal and recent historical development of the Po
975 river delta, Italy: in J. P Morgan and RH Shaver, eds., Deltaic Sedimentation Modern and Ancient:
976 SEP M. Spec. Publ. Am. Philos. Soc. 15, I52–184.

977 Nieuwenhuyse, A., 1996. Landscape formation and soil genesis in volcanic parent materials in humid
978 tropical lowlands of Costa Rica. Universiteit Wageningen.

979 Nieuwenhuyse, A., Kroonenberg, S.B., 1994. Volcanic origin of Holocene beach ridges along the
980 Caribbean coast of Costa Rica. Mar. Geol. 120, 13–26.

981 Pardo, N., Pulgarín, B., Betancourt, V., Lucchi, F. and Valencia, L.J., 2019. Facing geological mapping
982 at low-latitude volcanoes: The Doña Juana Volcanic Complex study-case, SW-Colombia. Journal
983 of Volcanology and Geothermal Research, 385, pp.46-67.

984 Pavanelli, N., Capaccioni, B., Sarocchi, D., Calderoni, G., Vaselli, O., Tassi, F., Duarte, E., 2004.
985 Geology and Stability of the Southern Flank of Irazu. Acta Vulcanologica 16, 1–7.

986 Peraldo, G., Mora, M., 2008. Enseñanzas de la actividad histórica de los volcanes Irazú y Turrialba,
987 Costa Rica, América Central, in: García-Acosta, V. (Ed.), Historia Y Desastres En América Latina,
988 Volumen III. Centro de Investigaciones y Estudios Superiores en Antropología Social / Red de
989 Estudios Sociales en Prevención de Desastres en América Latina (La Red), pp. 115–162.

990 Pérez-Consuegra, N., Hoyos, N., Restrepo, J. C., Escobar, J., & Hoke, G. D. (2021). Contrasting
991 climate controls on the hydrology of the mountainous Cauca River and its associated sedimentary
992 basin: Implications for interpreting the sedimentary record. Geomorphology, 377, 107590.

993 Pérez, W., Alvarado, G.E., Gans, P.B., 2006. The 322 ka Tiribí Tuff: Stratigraphy, geochronology and
994 mechanisms of deposition of the largest and most recent ignimbrite in the Valle Central, Costa
995 Rica. Bull. Volcanol. 69, 25–40.

996 Pierson, T.C., Major, J.J., 2014. Hydrogeomorphic Effects of Explosive Volcanic Eruptions on
997 Drainage Basins. Annu. Rev. Earth Planet. Sci. 42, 469–507.

998 Procter, J.N., Cronin, S.J., Zernack, A.V., 2009. Landscape and sedimentary response to catastrophic
999 debris avalanches, western Taranaki, New Zealand. Sediment. Geol. 220, 271–287.

1000 Quesada-Román, A., Fallas-López, B., Hernández-Espinoza, K., Stoffel, M., Ballesteros-Cánovas,
1001 J.A., 2019. Relationships between earthquakes, hurricanes, and landslides in Costa Rica.
1002 Landslides 16, 1539–1550.

1003 Radebaugh, J., Ventra, D., Lorenz, R.D., Farr, T., Kirk, R., Hayes, A., Malaska, M.J., Birch, S., Liu,
1004 Z.Y.-C., Lunine, J., Barnes, J., Le Gall, A., Lopes, R., Stofan, E., Wall, S., Paillou, P., 2018.
1005 Alluvial and fluvial fans on Saturn's moon Titan reveal processes, materials and regional geology.
1006 Geol. Soc. Spec. Publ. 440, 281–305.

1007 Rojas, V., Barahona, D., Alvarado, G.E., 2017. Geomorfología y petrografía de la colada Ángeles y
1008 del cono Monte de la Cruz, volcán Barva, Costa Rica. Revista Geológica de América Central 17–
1009 35.

Ruiz Cubillo, P., 2012. Reconstruction of the Paleo and Neo stages of Poás and Turrialba volcanoes, Costa Rica: Competing processes of growth and destruction. Rutgers, The State University of New Jersey, Ann Arbor, United States.

Ruiz-Cubillo, P., Vega-Salas, P., Barrantes-Jiménez, R., Loría-Salazar, L.G., 2015. Modelación de lahares generados por el Volcán Turrialba y su posible afectación a la red vial nacional. Programa Infraestructura del Transporte (PITRA), LanammeUCR.

Salgado, S., Ibarra, E., Mesén, R., 2016. De tierras altas a tierras bajas: propuesta y exploración de una ruta prehispánica y colonial en el Caribe de Costa Rica. Vínculos 37, 133–161.

Singh, A., Thomsen, K.J., Sinha, R., Buylaert, J.-P., Carter, A., Mark, D.F., Mason, P.J., Densmore, A.L., Murray, A.S., Jain, M., Paul, D., Gupta, S., 2017. Counter-intuitive influence of Himalayan river morphodynamics on Indus Civilisation urban settlements. Nat. Commun. 8, 1617.

Stanistreet, I.G., McCarthy, T.S., 1993. The Okavango Fan and the classification of suaerial fan system. Sediment. Geol. 85, 115–133.

van Ruitenbeek, F., 1994. Holocene, arc-volcanism controlled, episodic sedimentation in the atlantic lowland of Costa Rica. CATIE/AUW/MAG. Atlantic Zone Programme. Report No. 74. Field Report No. 120. Costa Rica. sp.

van Seeters, R.J.M., 1993. A study on geomorphology, mineralogy and geochemistry of the Toro Amarillo-Tortuguero and the Chirripo-Matina river system in the Atlantic Zone of Costa Rica. CATIE/AUW/MAG. Atlantic Zone Programme. Report No. 47. Field Report No. 95. Costa Rica. sp.

Ventra, D., Clarke, L.E., 2018. Geology and geomorphology of alluvial and fluvial fans: Current progress and research perspectives. Geol. Soc. Spec. Publ. 440. https://doi.org/10.1144/SP440.16

Vessell, R.K., Davies, D.K., 1981. Nonmarine Sedimentation in an Active Fore Arc Basin. https://pubs.geoscienceworld.org › books › book › chapterhttps://pubs.geoscienceworld.org › books › book › chapter. https://doi.org/10.2110/pec.81.31.0031

Villavicencio, E., 1885. Censo de población de Costa Rica 1883. Ministerio de Fomento. Sección de Estadística.

Villavicencio, E., 1893. Censo de población de Costa Rica 1892. Ministerio de Fomento. Sección de Estadística.

Weissmann, G. S., Adrian John Hartley, L. A. Scuderi, G. J. Nichols, A. Owen, S. Wright, A. L. Felicia, F. Holland, and F. M. L. Anaya, 2015. Fluvial geomorphic elements in modern sedimentary basins and their potential preservation in the rock record: a review. Geomorphology 250, 187-219.

Weissmann, G.S., Hartley, A.J., Nichols, G.J., 2010. Fluvial form in modern continental sedimentary basins: distributive fluvial systems.

Zani, H., Assine, M.L., McGlue, M.M., 2012. Remote sensing analysis of depositional landforms in alluvial settings: Method development and application to the Taquari megafan, Pantanal (Brazil). Geomorphology 161-162, 82–92.

Zhang, Y., Dai, X., Wang, M., Li, X., 2020. The concept, characteristics and significance of fluvial fans. Pet. Explor. Dev. 47, 1014–1026.